

**Supporting information for**  
**Glyco Star Polymers as a Helical Multivalent Host and Biofunctional Nano-Platform.**

Tomoki Nishimura<sup>1,2</sup>, Sada-atsu Mukai<sup>1,2</sup>, Shin-ichi Sawada<sup>1,2</sup>, and Kazunari Akiyoshi<sup>1,2\*</sup>

1. Department of Polymer Chemistry, Graduate School of Engineering, Kyoto University, Katsura, Nishikyo-ku, Kyoto 615-8510, Japan
2. ERATO Akiyoshi Bio nano transporter Project, Japan Science and Technology Agency (JST), Katsura Int'tech center, Kyotodaigakukatsura, Nishikyo, Kyoto 615-8530, Japan

**Contents**

**Materials and Methods**

- Figure S1 Photograph of the enzymatic polymerization mixture after incubating 24 hour at 5 degree
- Figure S2 <sup>1</sup>H-NMR spectra of C16SP with the glyco polymers and Changes in <sup>1</sup>H-NMR chemical shifts upon addition of with the glyco polymers.
- Figure S3 Hill plots for C16SP/ the glyco polymer system.
- Figure S4 <sup>1</sup>H-NMR spectra of Lyso PC with the glyco polymers and Changes in <sup>1</sup>H-NMR chemical shifts upon addition of with the glyco polymers.
- Figure S5 Hill plots for Lyso PC/ the glyco copolymers system.
- Figure S6 <sup>1</sup>H-NMR spectra of DMPC with the glyco polymers and Changes in <sup>1</sup>H-NMR chemical shifts upon addition of with the glyco polymers.
- Figure S7 Hill plots for DMPC/ the glyco polymers system.
- Table S1Hill coefficients and apparent binding constants for the lipid binding to the glyco polymers.
- Figure S8 The polymer concentration dependence of the UV-Vis profiles of OPV and Hill plots for OPV/the glyco polymers system.
- Figure S9 CD spectra of OPV and OPV/the glyco copolymers system.
- Figure S10 The polymer concentration dependence of the UV-Vis profiles of curcumin and Hill plots for curcumin/the polymers system.
- Figure S11 The polymer concentration dependence of the fluorescence profiles of BPP and Hill plots for BPP/the polymers system.
- Figure S12 The polymer concentration dependence of the fluorescence profiles of DPH.
- Figure S13 The polymer concentration dependence of the UV-Vis profiles of 6H.
- Figure S14 The polymer concentration dependence of the fluorescence profiles of Pyrene.
- Figure S15 The polymer concentration dependence of the fluorescence profiles of 2,6-ANS.
- Figure S16 The polymer concentration dependence of the fluorescence profiles of 1,8-ANS.
- Figure S17 Schematic drawing of the postulated amylose-lipid complex.
- Figure S18 Lineweaver-Burk plots for the cationic glyco star copolymers.

## **Synthetic Procedure**

- Figure S19 NMR spectra of azide functionalized 8 arm PEG.  
Figure S20 NMR spectra of azide functionalized 4 arm PEG.  
Figure S21 NMR spectra of Bis azide functionalized PEG.  
Figure S22 NMR spectra of Mono azide functionalized PEG.  
Figure S23 NMR spectra of maltopentaose functionalized 8 arm PEG.  
Figure S24 NMR spectra of maltopentaose functionalized 4 arm PEG.  
Figure S25 NMR spectra of Bis maltopentaose functionalized PEG.  
Figure S26 NMR spectra of Mono maltopentaose functionalized PEG.  
Figure S27 NMR spectra of Cat8Amy.  
Figure S28 NMR spectra of Cat4Amy.  
Figure S29 NMR spectra of Cat2Amy.  
Figure S30 NMR spectra of Cat1Amy.  
Figure S31 NMR spectra of ethyl 4-(hexadecyloxy)benzoate.  
Figure S32 NMR spectra of 4-(hexadecyloxy)benzoic acid.  
Figure S33 NMR spectra of C16SP.

## Materials

All starting materials were commercially available and were used without further purification. OPV is synthesized according to literature procedure<sup>[S1]</sup>. DNA oligonucleotides, 5'-TCA TAA TCA GCC ATA CCA CA-3' with and without FITC 3'-modification, and 5'-TGT GGT ATG GCT GAT TAT GA-3', with and without TAMRA 5'-modification, were purchased from FASMAC.

[S1]: N. Kato, et al, *Chem. Lett.* **2009**, 38, 1192-1193.

## Methods

### ***Estimation of the degree of polymerization with Inorganic phosphate assay:***

The reaction solution (10  $\mu$ L) was taken from the system at each reaction time. This was added to 2990  $\mu$ L of water and the solution was heated at 100 °C for 5 min. To 0.20mL of the solution, 0.80mL of molybdate reagent (15 mM ammonium molybdate, 100 mM zinc acetate, pH was adjusted to 5.0 with 2 M HCl solution), and 0.20 mL of sodium ascorbic acid solution (10 wt %, PH=5.0) were added. The mixture was incubated at 30 °C for 15 min. The absorption of these solutions was measured with a JASCO V-570 spectrometer set to scan the 600–900 nm wavelength range. Samples were analyzed in a 10 mm quartz cuvette.

### ***Preparation of the star polymer-based hydrogel:***

To a solution of primer (0.93  $\mu$ mol/maltopentaose), glucose-1-phosphate (85 mg, 0.27 mmol), and adenosine mono phosphate (34 mg, 0.1 mmol) in Bis tris buffer (pH=6.0; 0.1 M), rabbit muscle Phosphorylase b (0.36 mg) was added. Then the solution was incubated at 40 °C for 24 hour. Then the solution was allowed to stand at 5 °C for 24 hour. Gelation was confirmed with tube inversion test.

### ***Complex Formation of Iodine with glyco copolymers:***

Standard iodine-iodide solution (5 g of KI, 0.2 g of I<sub>2</sub> in 250 ml; 40  $\mu$ l) and polymer solution (40  $\mu$ l, 1.21 mM) were mixed and diluted with water to 4.0 ml. The absorption of these solutions was measured with a JASCO V-570 spectrometer set to scan the 300–900 nm wavelength range. Samples were analyzed in a 1 cm quartz cuvette.

### ***Complex Formation of the hydrophobic probes with glyco polymers:***

Stock solutions of glyco polymers (1 mM) and the probes (1 mM) were prepared in a 98 : 2 (v: v) mixture of PBS buffer solution (pH=7.2) and DMSO. The resultant glyco polymer solution was added to an appropriate amount of the probe solution (1.0  $\times$  10<sup>-6</sup> M for fluorescence probes, 1.2  $\times$  10<sup>-5</sup> M for OPV, 5.0  $\times$  10<sup>-6</sup> M for curcumin and 6T). In the case of 6T, we used a 95 : 5 (v: v) mixture of PBS buffer and THF. UV-Vis or fluorescence spectra were collected after incubation for 30 min. The UV-Vis and fluorescence measurements were carried out with a UV-Vis spectrophotometer (JASCO V-570) and fluorescence spectrophotometer (JASCO FP-6500 spectrometer), respectively. The solutions were put into a quartz cell with the thickness of 10 mm, and the spectrum was obtained at 25 °C at a scanning speed of 200 nm min<sup>-1</sup>. The excitation wavelength of the probes was as follows;

DPH: 350nm, BPP: 339nm, Pyrene: 335nm, 1,8-ANS: 350nm, 2,6-ANS: 320nm

### ***Complex formation of the lipids with glyco polymers:***

The CMC value of C16SP was determined to be 0.25 mM. Therefore, NMR titration experiment was performed at concentrations above its CMC. Stock solutions of glyco polymers (16 mM) and C16SP (0.69 mM) were prepared in a 99 : 1 (v : v) mixture of D<sub>2</sub>O and d<sub>6</sub>-DMSO. In the case of DMPC and Lyso PC, stock solutions of the lipids were prepared in a 94 : 5 : 1 (v : v : v) mixture of D<sub>2</sub>O, d<sub>4</sub>-MeOH, and d<sub>6</sub>-DMSO. An appropriate amount of glyco copolymer solution were added to the C16SP solution and gently shaken by hand. NMR spectra were corrected after incubation for 15 min. NMR spectra were measured at 400 MHz on a Bruker avance spectrometer at 298 K and recorded with a total of 16.4 k data points, 64 scans, and a recycle delay of 4 s. The change in chemical shift ( $\Delta\delta$ ) of the CH<sub>3</sub> protons of terminal alkyl chain were monitored and fitted to hill equation (eq 1) to determine the hill coefficient (h) and the association constant (K<sub>a</sub>)

$$\log[Y/1-Y] = h \log [X] + h \log K_a \text{ (eq 1)}$$

$$Y = (\Delta\delta_{\text{obs}} - \Delta\delta_{\text{initial}}) / (\Delta\delta_{\text{infinite}} - \Delta\delta_{\text{obs}})$$

[X] : the concentration of polymer

$K_a$  = overall association constant

### DNA strand exchange experiments:

Strand exchange kinetics were monitored through FRET assay using DNA duplexes labeled with FITC on the 3' end of one strand and TAMRA on the 5' end of the other. The doubly labeled ds-DNA does not show the fluorescence emission from FITC because FRET pair is in close proximity. The ds-DNA is mixed with 10 folds unlabeled ss-DNA, which is complementary to the FITC modified DNA, in the absence and in the presence of cationic compounds. The FITC emission increases when the stands are exchanged due to the separation of the FRET pair. To form duplexes, equimolar amounts of complementary strands were heated to 95°C and annealed slowly over six hours. A stirred solution of FRET-labeled ds-DNA mixed with each polymer (spermamine groups in polymer/phosphate groups in DNA ratio = 10) was allowed to equilibrate to 25°C. Final concentration of the ds-DNA was 2.4 nM, dissolved in 50 mM Tris-sulfate (pH=7.2), containing 150 mM NaCl, 0.5 mM EDTA. The solution was excited at 490 nm and fluorescence emission at 520 nm was monitored with a JASCO FP-6500 spectrometer equipped with a temperature-controlled cell holder. Baseline emission values were first recorded for 1 min, and then the ss-DNA solution (final concentration: 12 nM) was injected to initiate strand exchange reaction. The value of % exchange degree was calculated with following equation (eq 2):

% Exchange degree

$$= ([FI]_t - [FI]_0) / ([FI]_{\text{ref}} - [FI]_0) \times 100 \text{ (eq 2)}$$

where  $[FI]_0$  is the initial fluorescence intensity,  $[FI]_t$  and  $[FI]_{\text{ref}}$  are fluorescence intensity at time t and after the reaction reached equilibrium, respectively. The reference sample was prepared by mixing the same amounts of double- and single-stranded DNA as in the kinetic experiments. The mixture was heated to 90°C and slowly cooling it. The values of  $[FI]_{\text{ref}}$  of the reference samples were measured in the presence of polymers. Apparent rates of the exchange reaction were determined by pseudo first-order kinetic analysis (eq 3).

$k't$

$$= -\ln(\text{exchange degree \%} / 1000) \text{ (eq 3)}$$

### Michaelis-Menten analysis:

The exchange activity assays were performed by measuring the initial exchange rates. Because the fluorescence intensity is affected by changing the concentration of the substrate, we used a constant substrate concentration rather than a constant polymer concentration. The kinetic parameters were determined by using the Michaelis-Menten approach, through the equation 4:

$$V/[S_0] = k_{\text{cat}}[E]/(K_d + [E]) \text{ (eq 4)}$$

where V is the initial reaction rate,  $[S_0]$  the total substrate concentration, and  $[E]$  concentration of spermamine groups. The kinetic parameters  $k_{\text{cat}}$  and  $K_d$  were determined from a Lineweaver-Burk plot of  $1/V$  vs  $1/[E]$  using a linear least-squares fit of the experimental data.

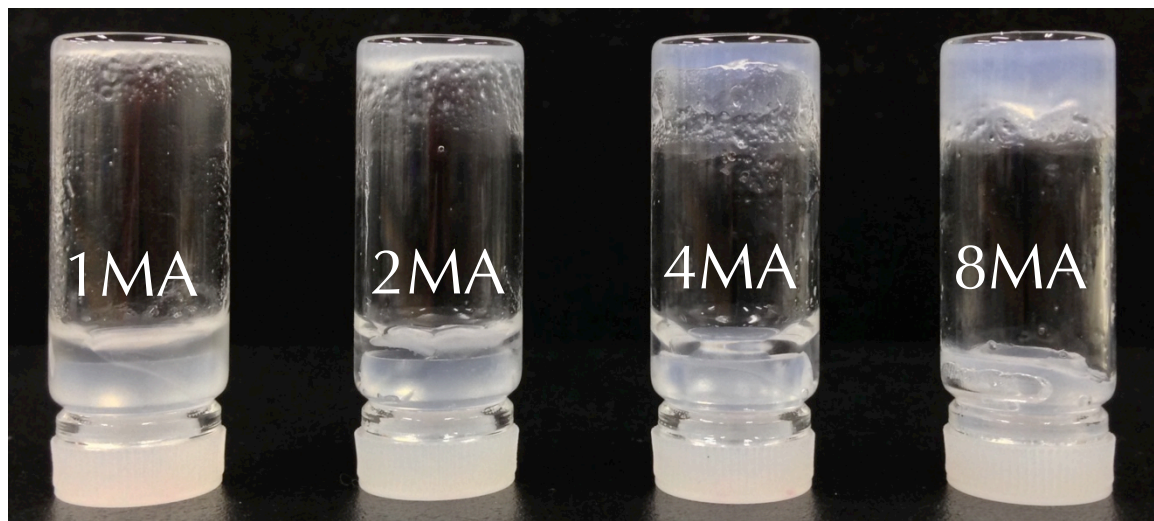


Figure S1 Photograph of the enzymatic polymerization mixture for the polymers after incubating 24 hour at 5 degree.

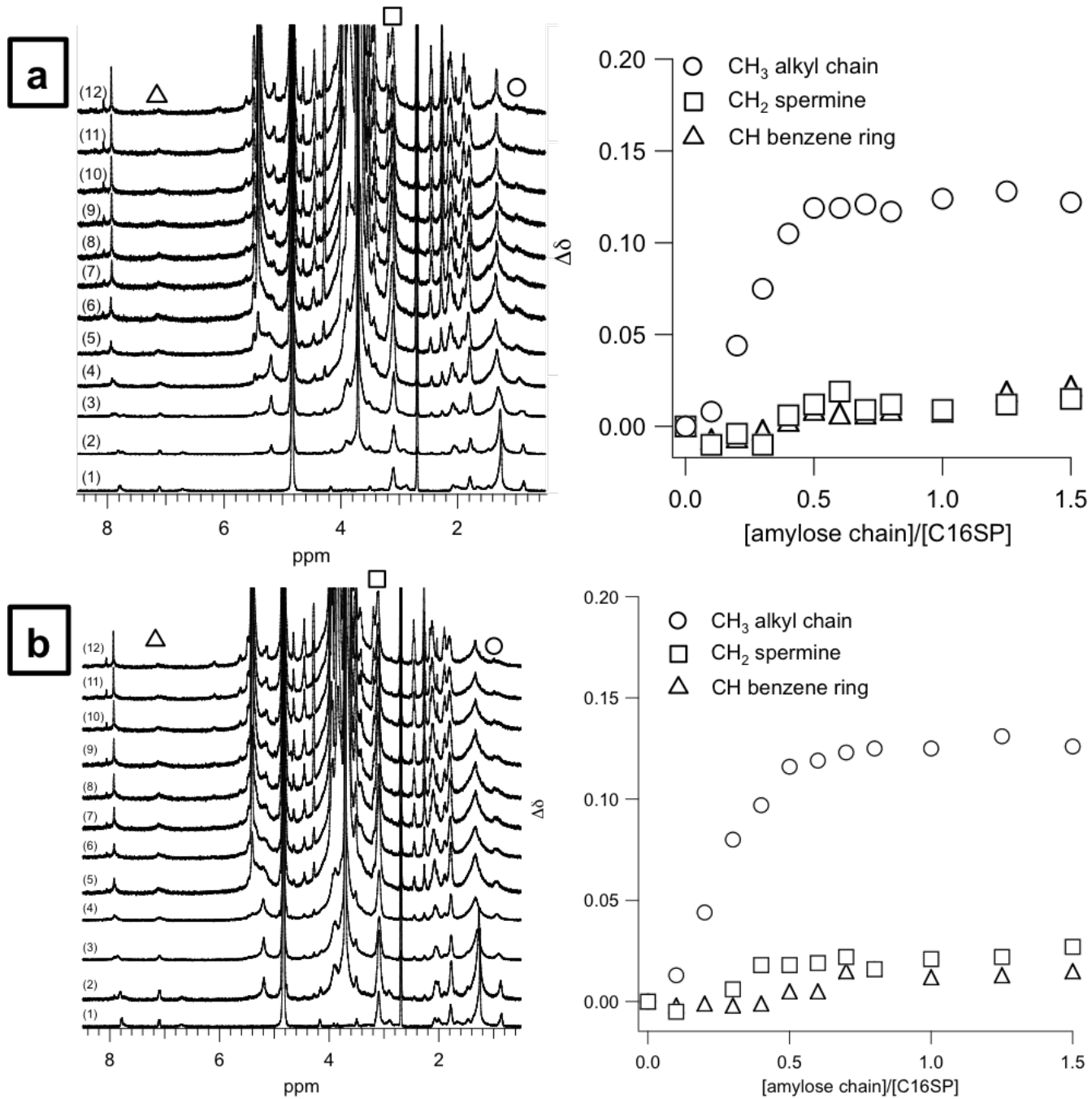
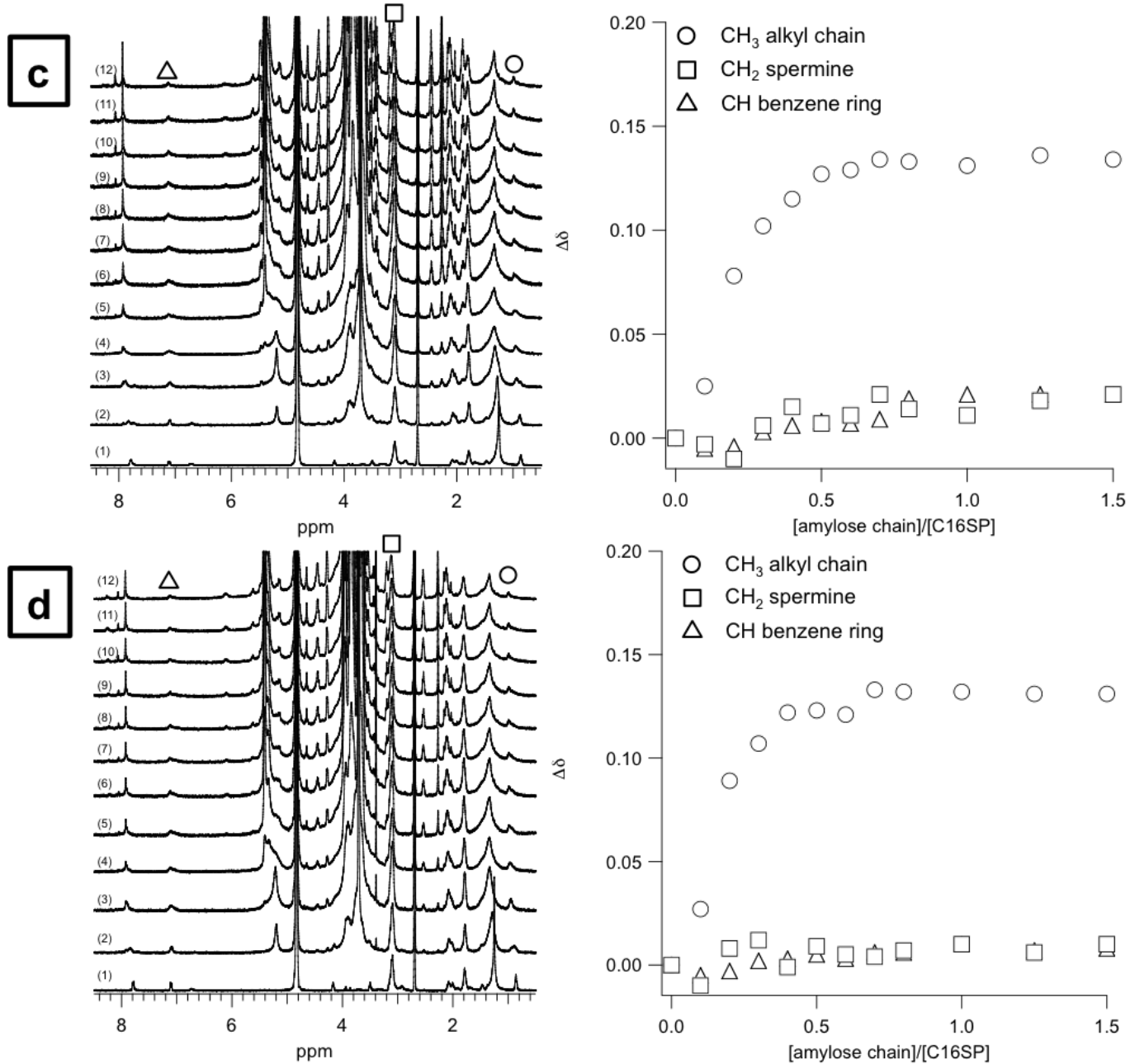


Figure S2-1 (left)  $^1\text{H}$ -NMR spectra in a 95 : 5 (v: v) mixture of  $\text{D}_2\text{O}$  and  $\text{d}_6\text{-DMSO}$  of (1) C16SP (0.69 mM) with the glyco polymers: (2) 0.069 mM, (3) 0.138 mM, (4) 0.207 mM, (5) 0.276 mM, (6) 0.345 mM, (7) 0.414 mM, (8) 0.483 mM, (9) 0.552 mM, (10) 0.690 mM, (11) 0.863 mM, (12) 1.04 mM. (right) Changes in  $^1\text{H}$ -NMR chemical shifts for  $\text{CH}_3$ (alkylchain),  $\text{CH}_2$ (spermine), and CH(benzene ring) of C16SP upon addition of the polymers. (a):8Amy, (b):4Amy



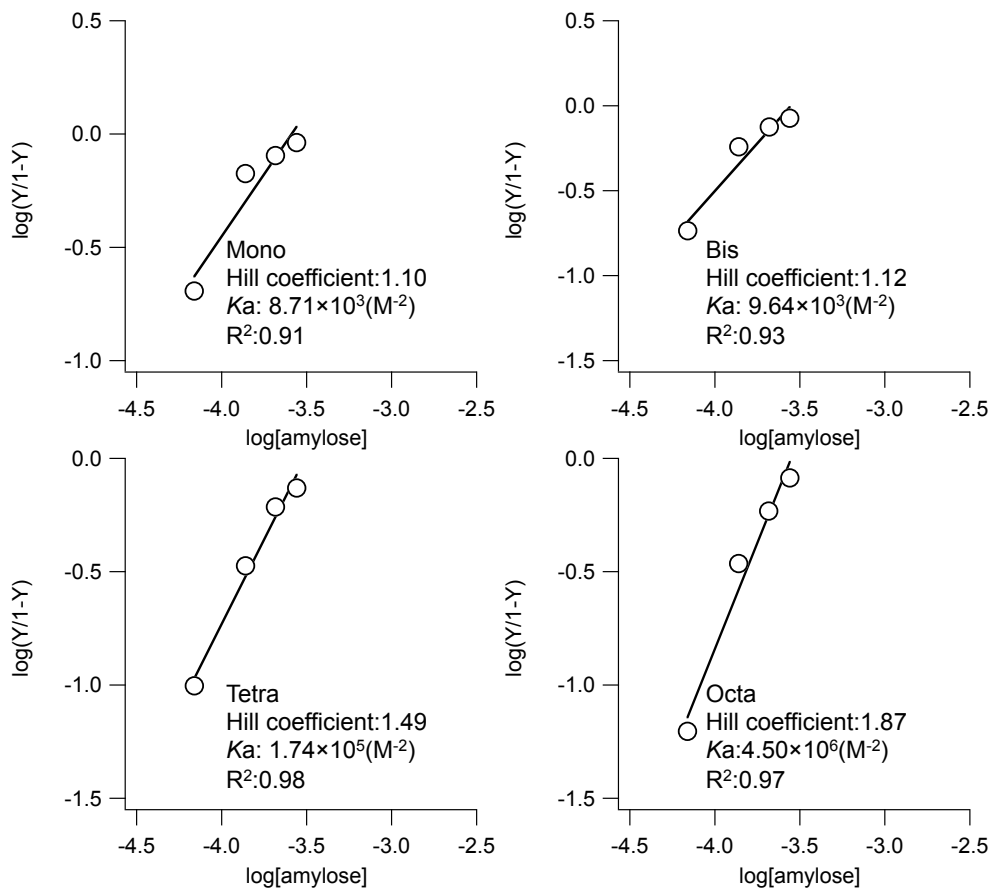


Figure S3 Hill plots from  $^1\text{H-NMR}$  titrations for C16SP/glyco polymers system.

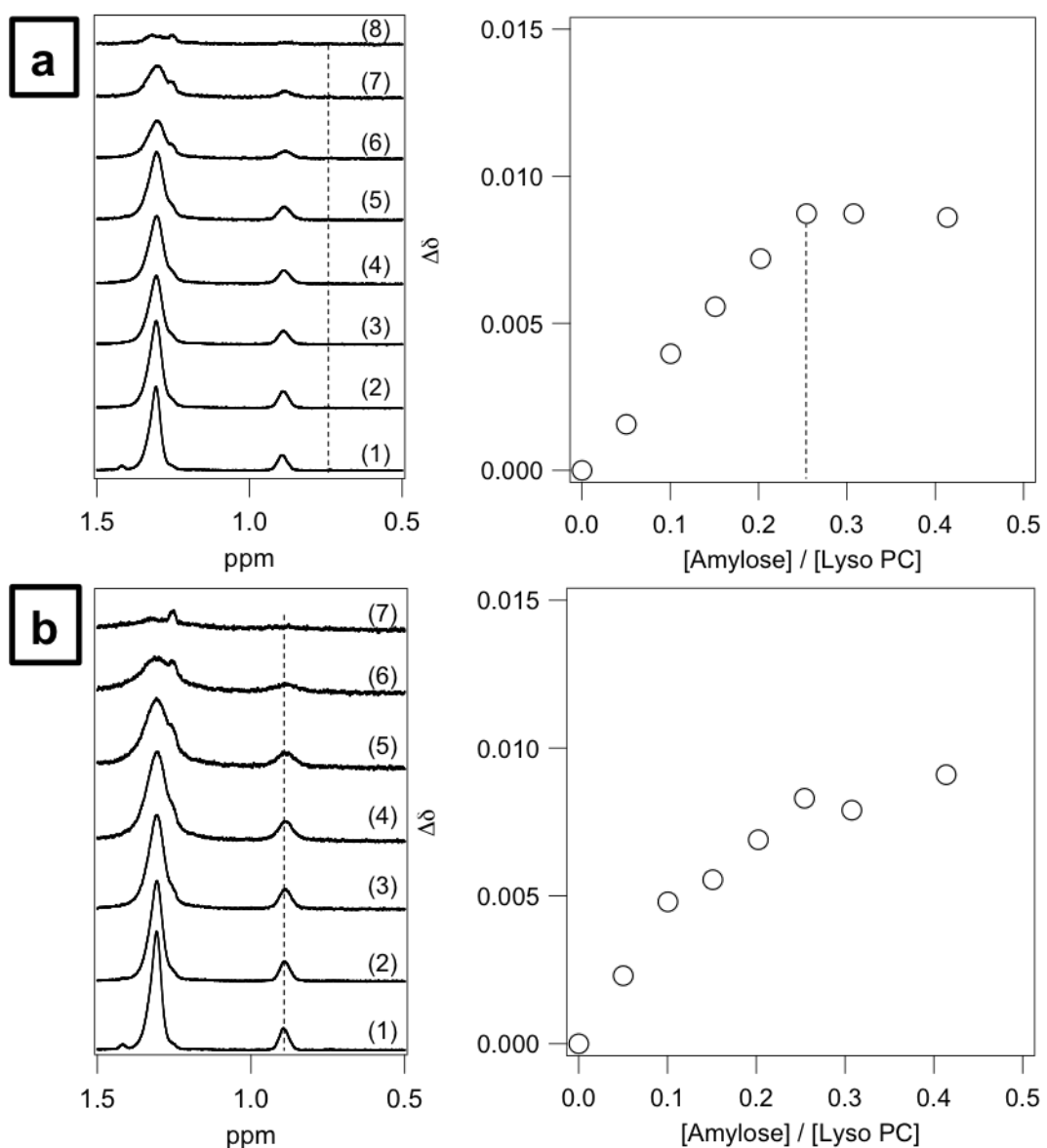


Figure S4-1 (left) <sup>1</sup>H-NMR spectra in a 94 : 5 : 1 (v : v : v) mixture of D<sub>2</sub>O, d<sub>4</sub>-MeOH, and d<sub>6</sub>-DMSO of (1) Lyso PC (0.75 mM) with the glyco polymer: (2) 0.037 mM, (3) 0.075 mM, (4) 0.112 mM, (5) 0.150 mM, (6) 0.186 mM, (7) 0.223 mM, (8) 0.297 mM. (right) Changes in <sup>1</sup>H-NMR chemical shifts of CH<sub>3</sub>(alkyl chain) of Lyso PC upon addition of with the glyco polymer. (a):8Amy, (b):4Amy

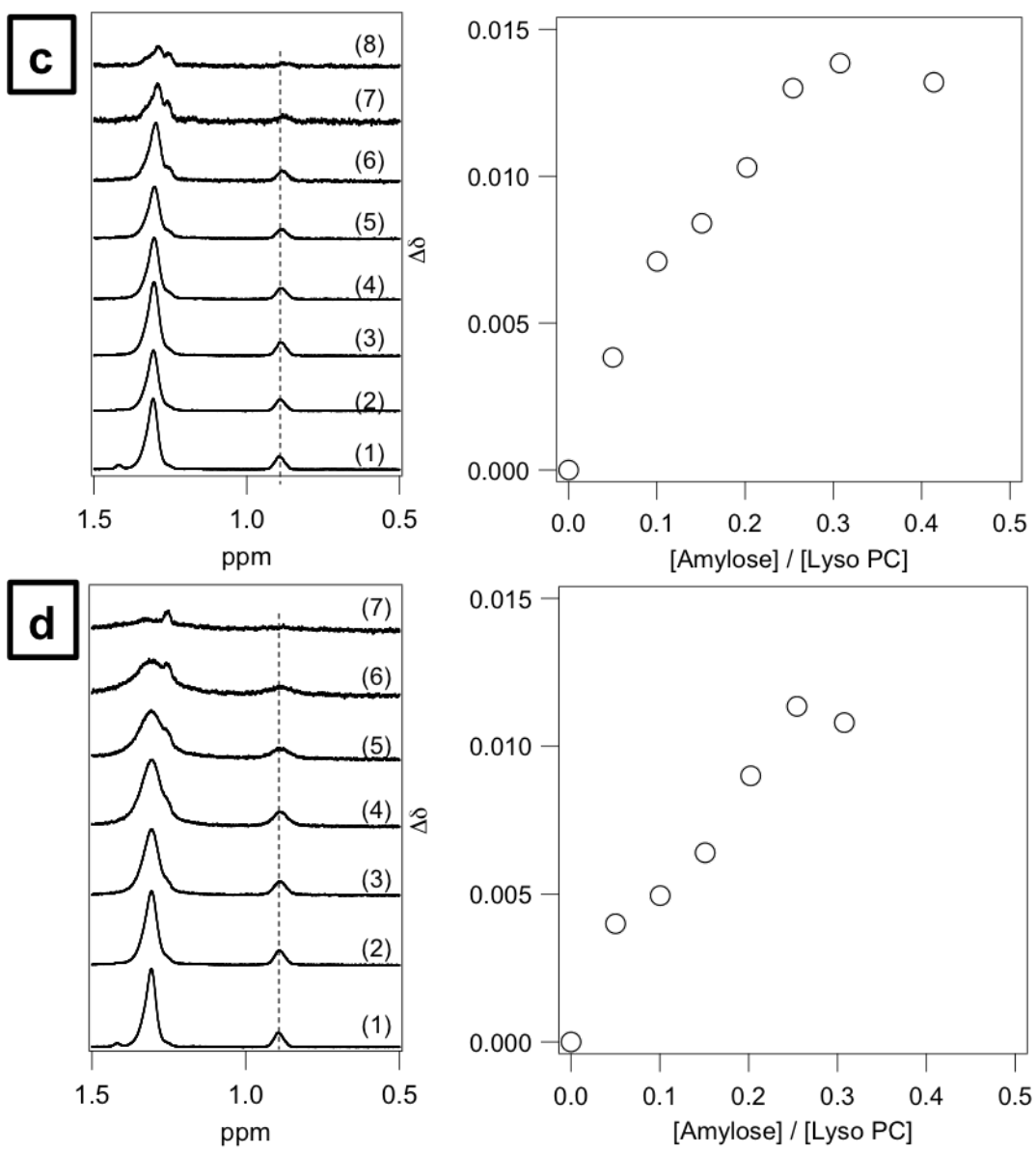


Figure S4-2 (left)  $^1\text{H}$ -NMR spectra in a 94 : 5 : 1 (v : v : v) mixture of  $\text{D}_2\text{O}$ ,  $d_4\text{-MeOH}$ , and  $d_6\text{-DMSO}$  of (1) Lyso PC ( 0.75 mM) with the glyco polymer: (2) 0.037 mM, (3) 0.075 mM, (4) 0.112 mM, (5) 0.150 mM, (6) 0.186 mM, (7) 0.223 mM, (8) 0.297 mM. (right) Changes in  $^1\text{H}$ -NMR chemical shifts of  $\text{CH}_3$ (alkyl chain) of Lyso PC upon addition of with the glyco polymer. (c) 2Amy, (d) 1Amy

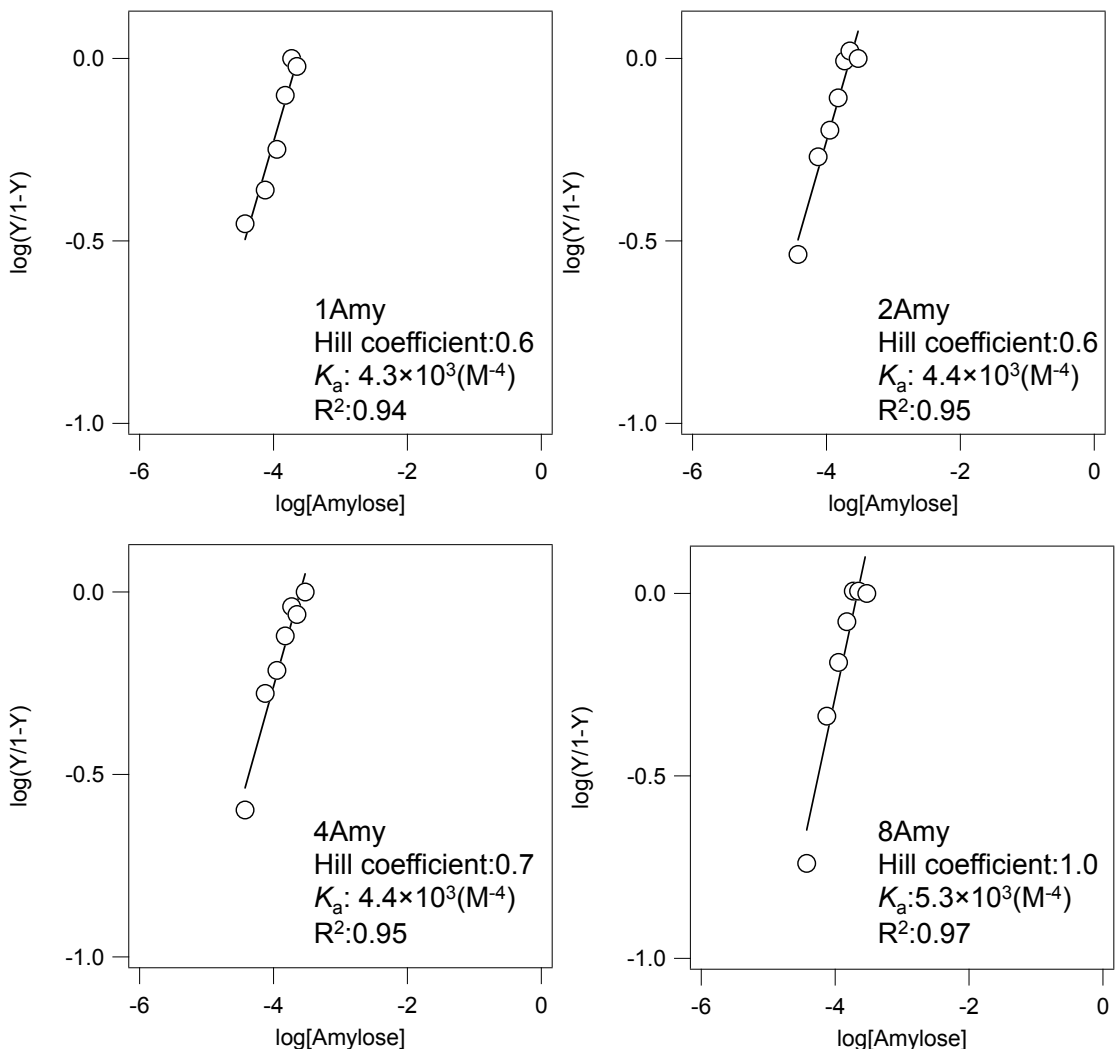


Figure S5 Hill plots from  $^1\text{H}$ -NMR titrations for Lyso PC/glyco polymers system.

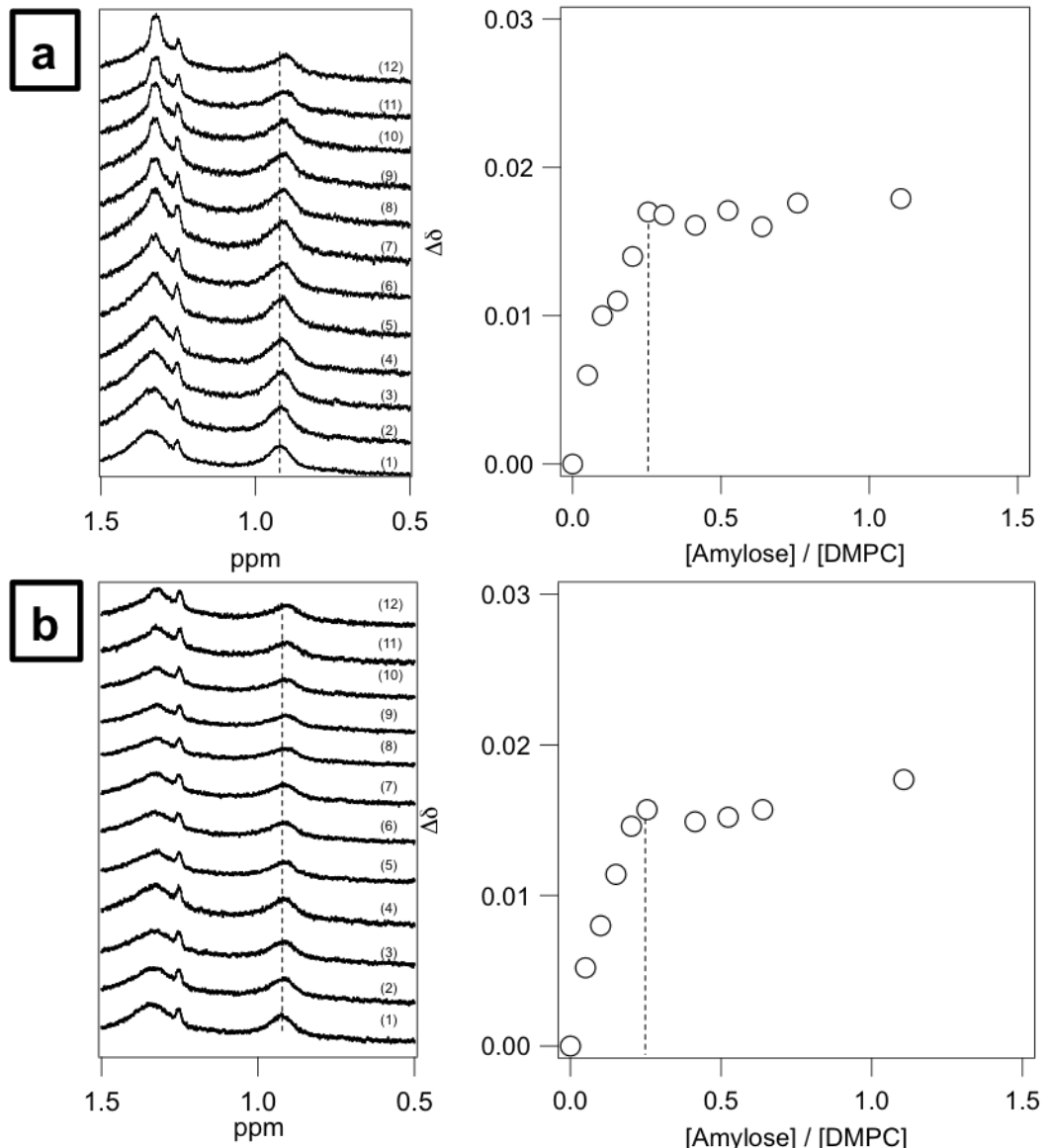


Figure S6-1 (left)  $^1\text{H}$ -NMR spectra in a 94 : 5 : 1 (v : v : v) mixture of  $\text{D}_2\text{O}$ ,  $d_4\text{-MeOH}$ , and  $d_6\text{-DMSO}$  of (1) DMPC (0.75 mM) with the glyco polymer: (2) 0.0375 mM, (3) 0.0748 mM, (4) 0.112 mM, (5) 0.149 mM, (6) 0.186 mM, (7) 0.223 mM, (8) 0.297 mM, (9) 0.370 mM, (10) 0.442 mM, (11) 0.515 mM, (12) 0.728 mM. (right) Changes in  $^1\text{H}$ -NMR chemical shifts of  $\text{CH}_3$ (alkyl chain) of DMPC upon addition of with the glyco polymer. (a):8Amy, (b):4Amy

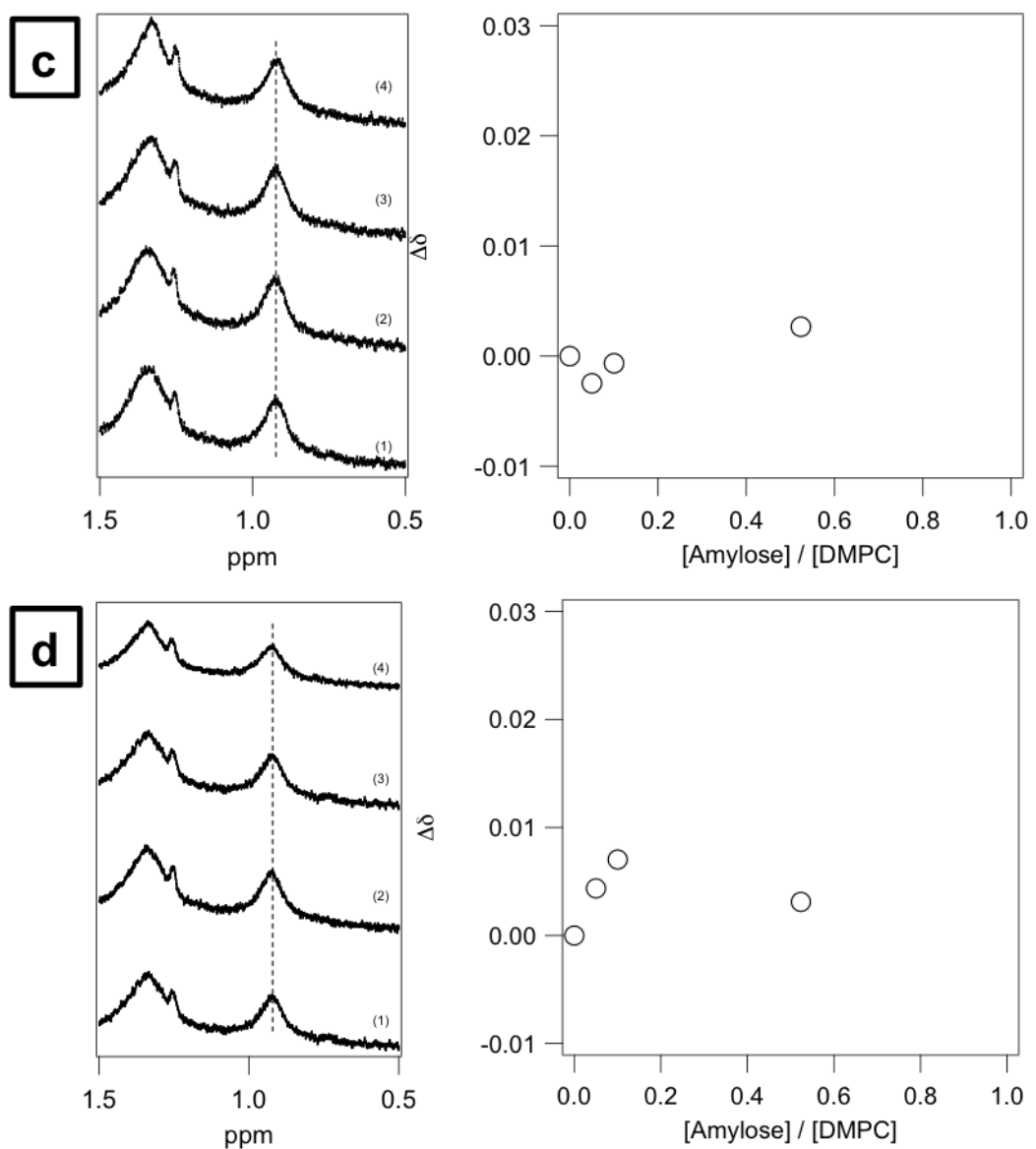


Figure S6-2 (left)  $^1\text{H}$ -NMR spectra in a  $94 : 5 : 1$  ( $\text{v} : \text{v} : \text{v}$ ) mixture of  $\text{D}_2\text{O}$ ,  $d_4\text{-MeOH}$ , and  $d_6\text{-DMSO}$  of (1) DMPC (0.75 mM) with the glyco polymer: (2) 0.0375 mM, (3) 0.0748 mM, (4) 0.112 mM, (5) 0.149 mM, (6) 0.186 mM, (7) 0.223 mM, (8) 0.297 mM, (9) 0.370 mM, (10) 0.442 mM, (11) 0.515 mM, (12) 0.728 mM. (right) Changes in  $^1\text{H}$ -NMR chemical shifts of  $\text{CH}_3$ (alkyl chain) of DMPC upon addition of with the glyco polymer. (c):2Amy, (d):1Amy

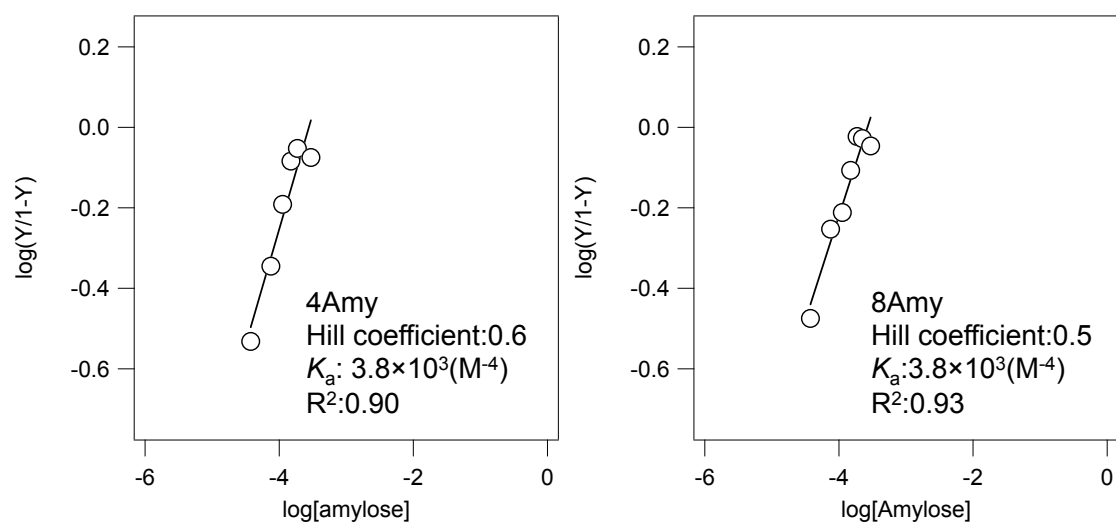


Figure S7 Hill plots from  $^1\text{H-NMR}$  titrations for DMPC/glyco polymers system.

Table S1. Hill coefficients and apparent binding constants for the lipid binding to the polymers

	Polymer	Hill coefficient	Binding constant
C16SP	1Amy	1.1	$9.6 \times 10^3 \text{ (M}^{-2}\text{)}$
	2Amy	1.1	$1.1 \times 10^4 \text{ (M}^{-2}\text{)}$
	4Amy	1.5	$2.6 \times 10^5 \text{ (M}^{-2}\text{)}$
	8Amy	1.9	$8.4 \times 10^6 \text{ (M}^{-2}\text{)}$
LysoPC	1Amy	0.6	$4.3 \times 10^3 \text{ (M}^{-4}\text{)}$
	2Amy	0.6	$4.4 \times 10^3 \text{ (M}^{-4}\text{)}$
	4Amy	0.7	$4.4 \times 10^3 \text{ (M}^{-4}\text{)}$
	8Amy	1.0	$5.3 \times 10^3 \text{ (M}^{-4}\text{)}$
DMPC	1Amy	- <sup>a</sup>	- <sup>a</sup>
	2Amy	- <sup>a</sup>	- <sup>a</sup>
	4Amy	0.6	$3.8 \times 10^3 \text{ (M}^{-4}\text{)}$
	8Amy	0.5	$3.8 \times 10^3 \text{ (M}^{-4}\text{)}$

a: no binding observed

#### The influence of lipid types on the binding affinity.

##### 1. The effect of the number of alkyl chain

DMPC vs. LysoPC

The number of alkyl chain has influence on the stability of the complex. The higher the number of alkyl chain, the lower the stability of the resulting complex. This can be explained that the diameter of amylose helix does not fit bulkier compounds. The binding affinity for LysoPC is slightly larger than that of DMPC (ex. LysoPC/8Amy vs DMPC/8Amy). Since DMPC molecule is bulkier than LysoPC, such steric configuration is responsible for the decrease of the binding affinity.[S2,S3]

[S2]: Eliasson et al. Thermochim. acta 1994, 246, 343

[S3]: Cesar et al. Carbohydr. Res. 2012, 364, 1

##### 2. The effect of the alkyl chain length

C16SP vs. LysoPC

The longer alkyl chain of lipids allows more hydrophobic interactions with the interior of the amylose helix, resulting in the formation of stable complex. The C16SP/polymer complexes were more stable than those with LysoPC/polymer complexes. This can be explained by the longer hydrocarbon chain allows more hydrophobic interaction with the interior of the amylose helix.[S4]

[S4]: Gelders et al. Biomacromolecules 2005, 6, 2622

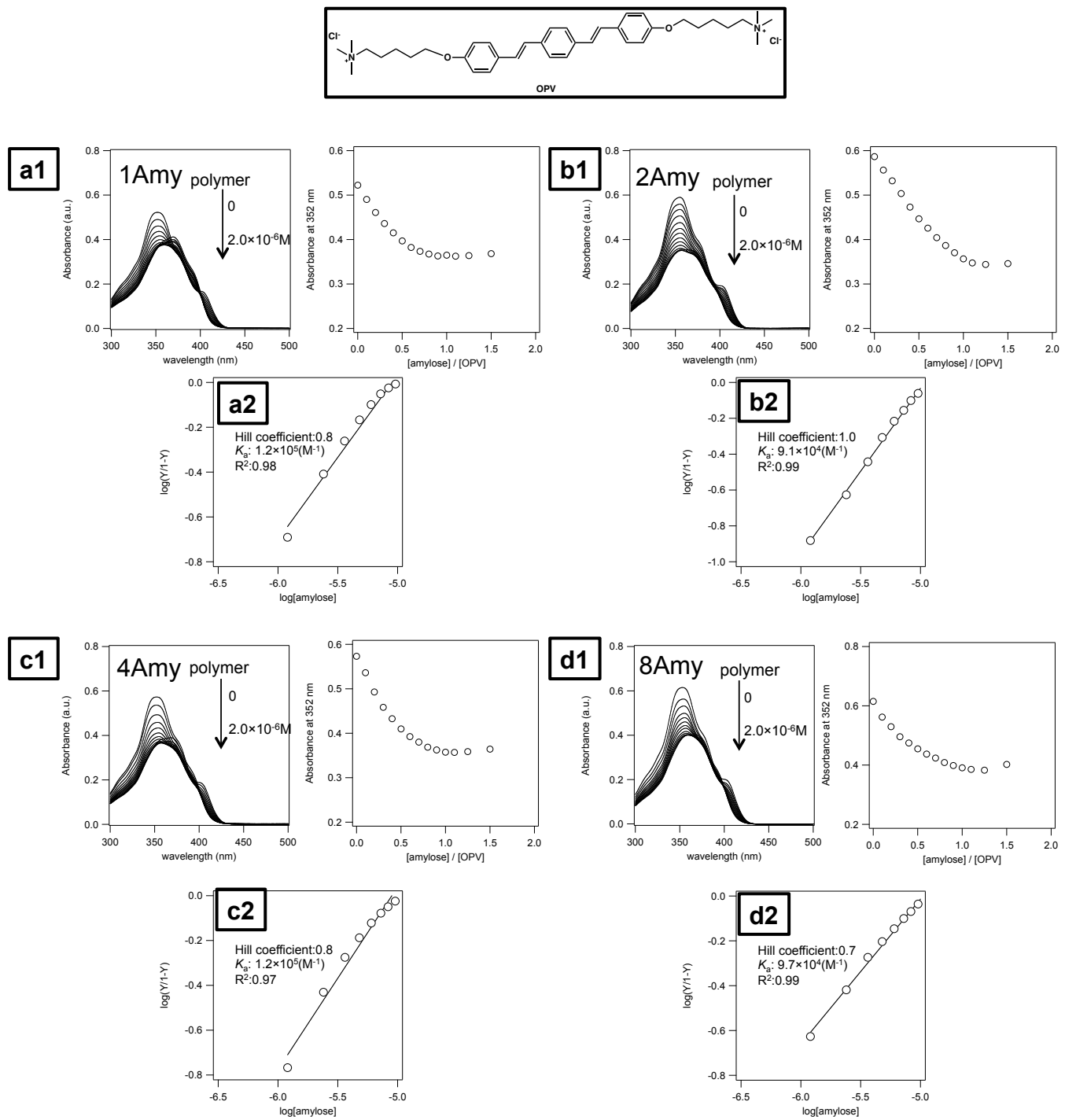


Figure S8 (a1–d1) The glyco copolymer concentration dependence of the UV-Vis profiles of OPV. The absorbance at 352 nm plotted against molar ratio. (a2–d2) Hill plots from UV-Vis titrations for OPV/glyco polymer system.

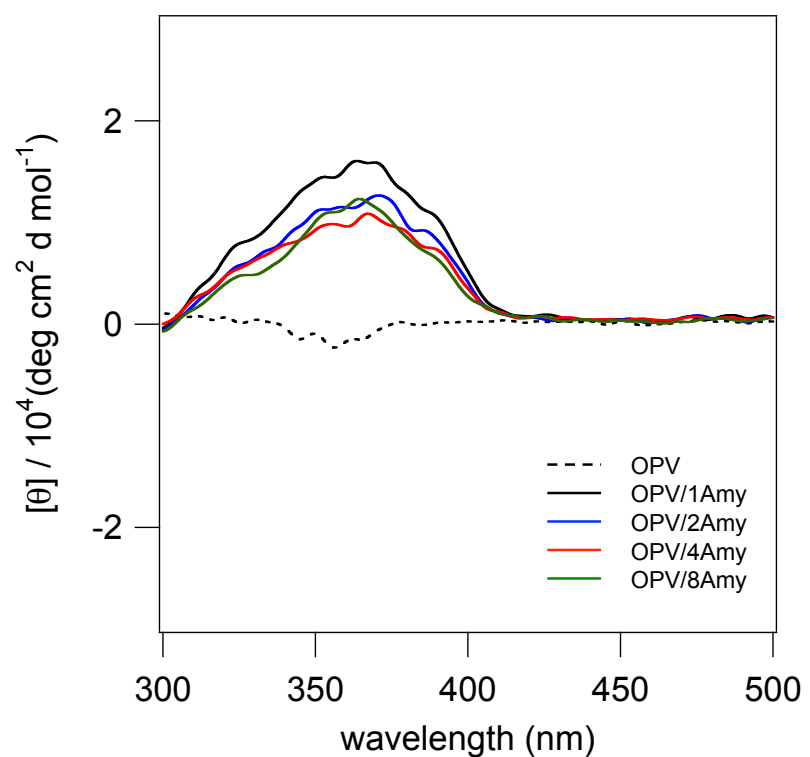


Figure S9 CD spectra of OPV and OPV/glyco polymers system.

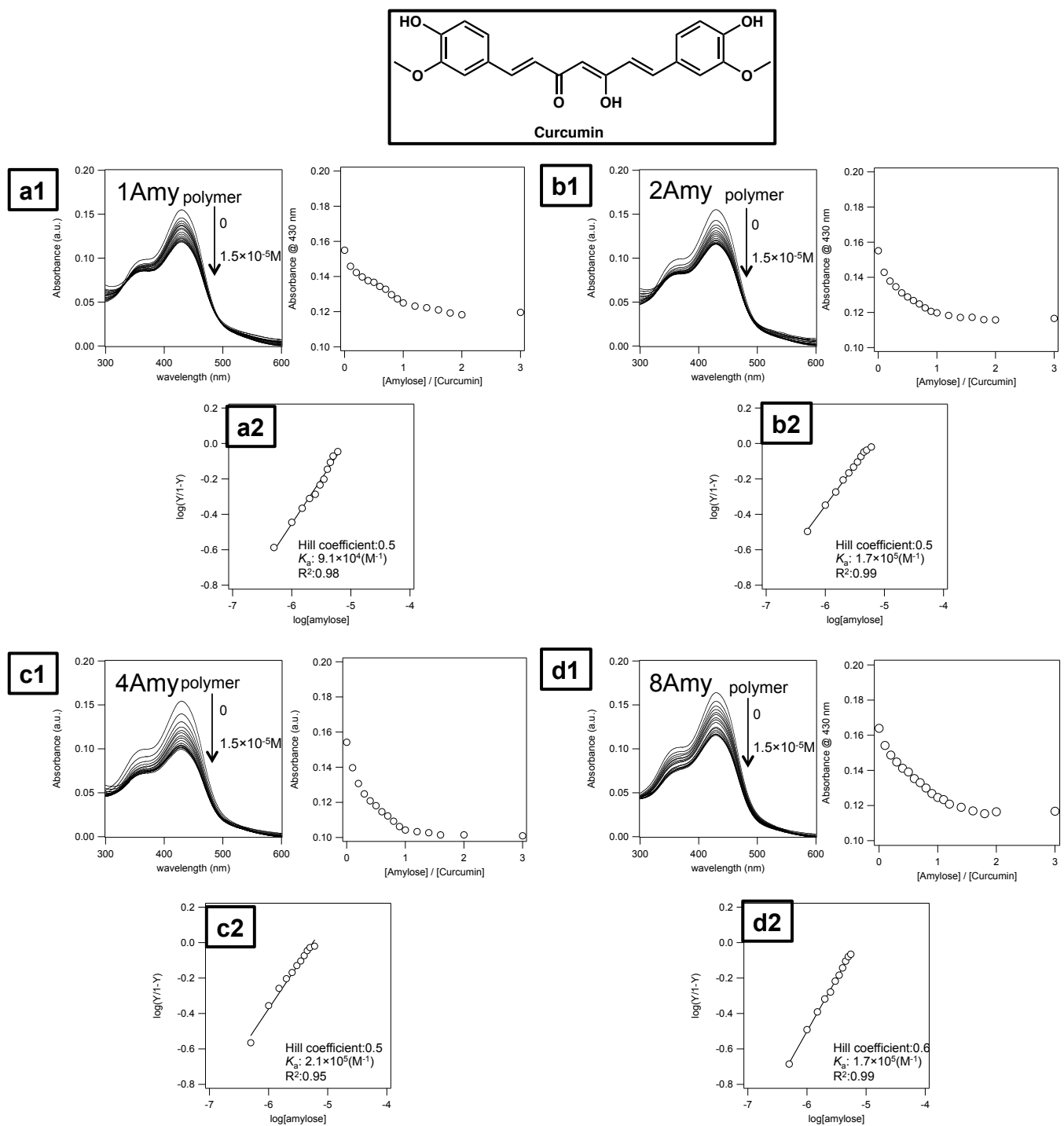


Figure S10 (a1–d1) The glyco copolymer concentration dependence of the UV-Vis profiles of curcumin. The absorbance at 430 nm plotted against molar ratio. (a2–d2) Hill plots from UV-Vis titrations for curcumin/glyco polymers system.

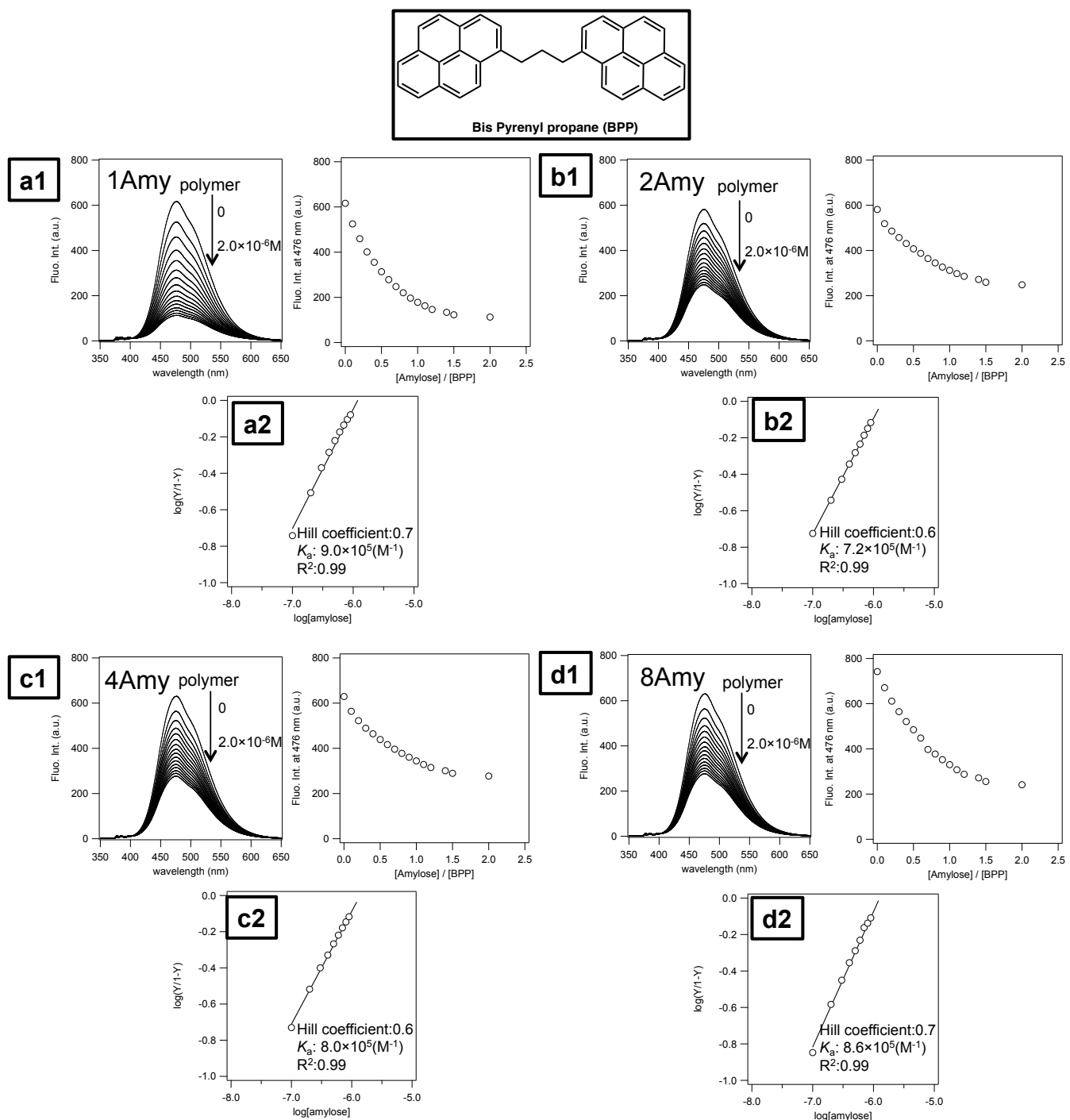


Figure S11 (a1–d1) The glyco polymer concentration dependence of the fluorescence profiles of BPP. The relative fluorescence intensity at 476 nm plotted against molar ratio. (a2–d2) Hill plots from UV-vis titrations for BPP/glyco polymers system.

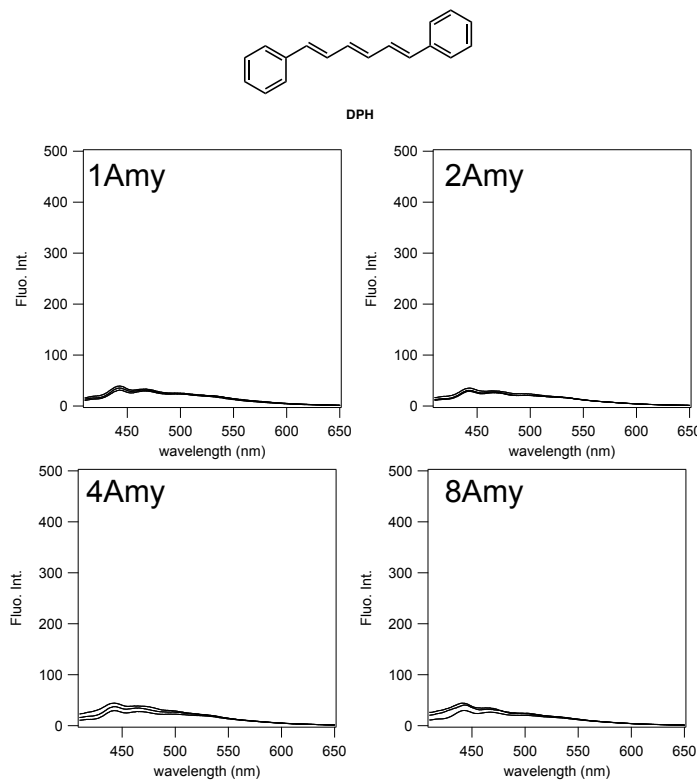


Figure S12 The glyco copolymer concentration dependence of the fluorescence profiles of DPH. Polymer concentrations: 0,  $0.5 \times 10^{-6}$  M, and  $1.0 \times 10^{-6}$  M. [DPH] =  $1.0 \times 10^{-6}$  M.

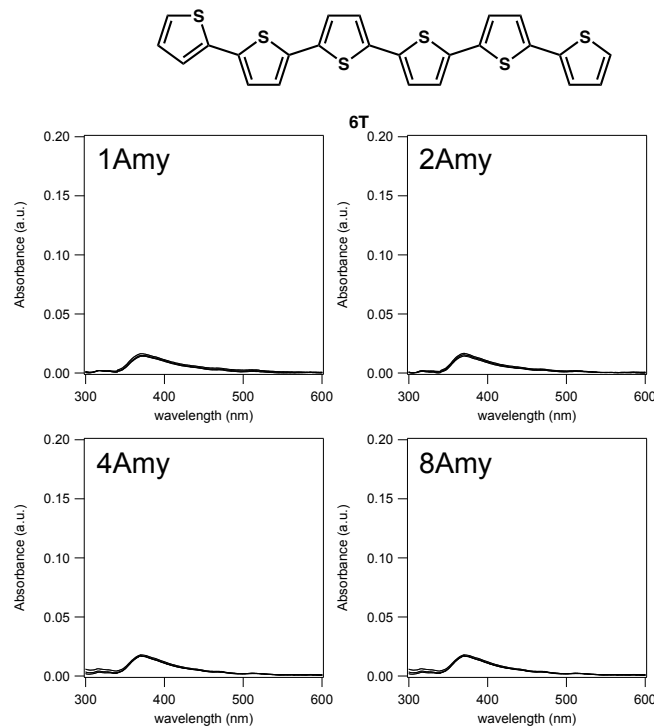


Figure S13 The glyco copolymer concentration dependence of the UV-Vis profiles of 6T. Polymer concentrations: 0,  $2.5 \times 10^{-6}$  M, and  $5.0 \times 10^{-6}$  M. [6T] =  $5.0 \times 10^{-6}$  M.

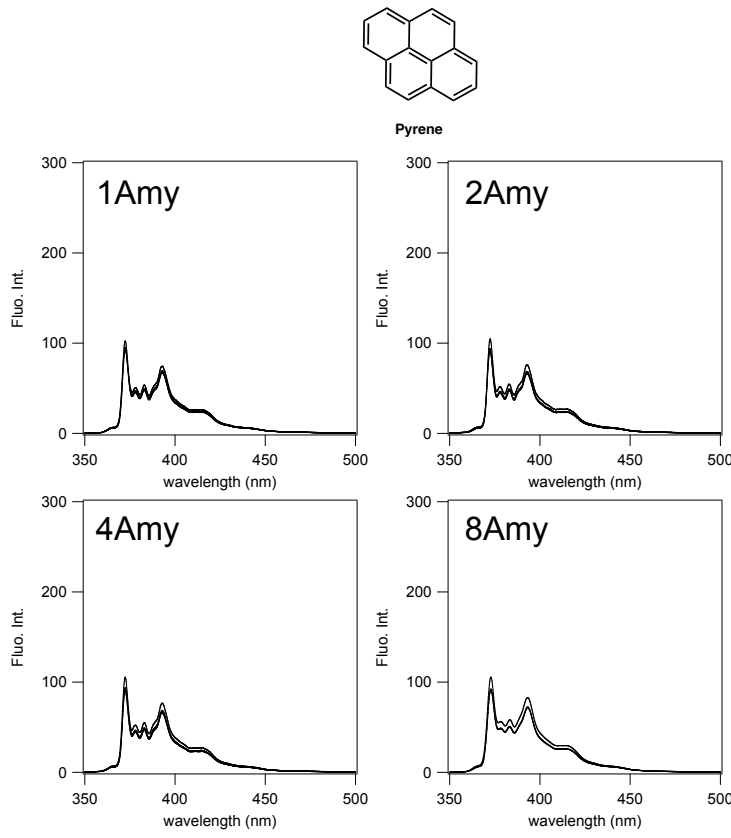


Figure S14 The glyco copolymer concentration dependence of the fluorescence profiles of Pyrene. Polymer concentrations: 0,  $1.0 \times 10^{-6}$  M, and  $2.0 \times 10^{-6}$  M. [Pyrene] =  $1.0 \times 10^{-6}$  M.

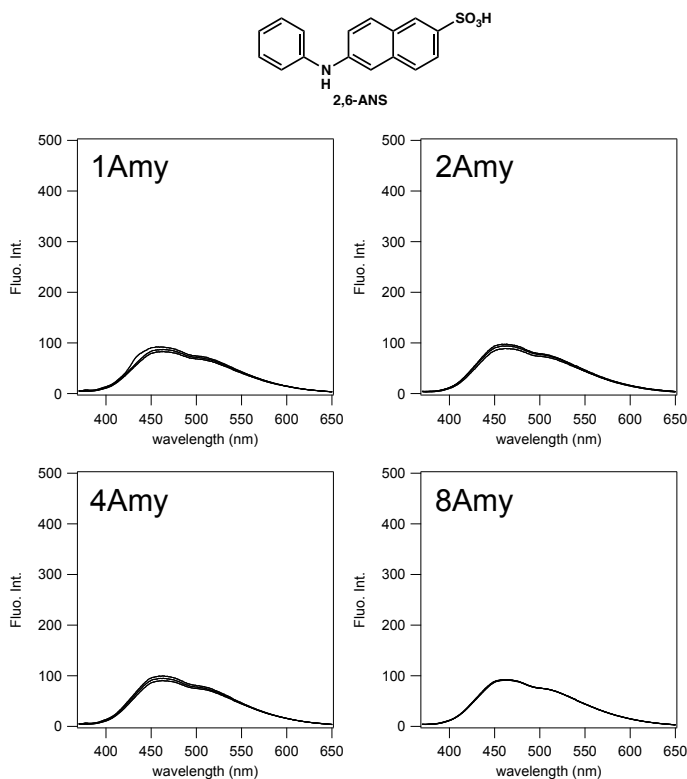


Figure S15 The glyco copolymer concentration dependence of the fluorescence profiles of 2,6-ANS. Polymer concentrations: 0,  $2.5 \times 10^{-6}$  M, and  $5.0 \times 10^{-6}$  M. [2,6-ANS] =  $5.0 \times 10^{-6}$  M.

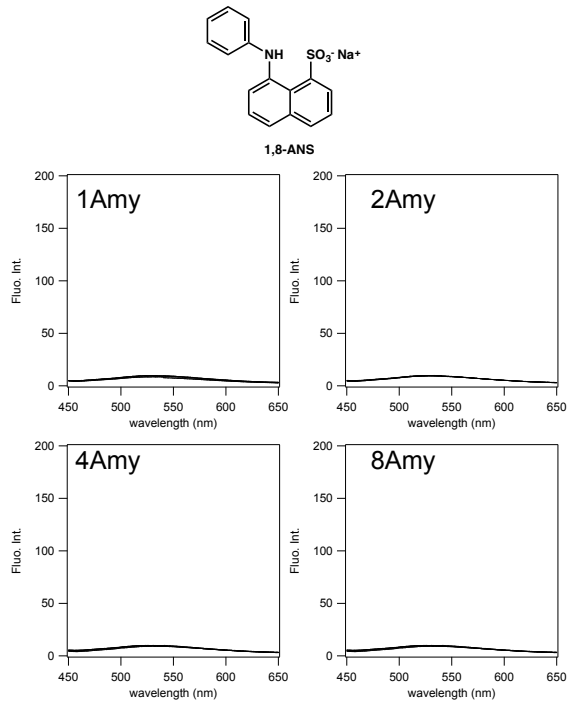


Figure S16 The glyco copolymer concentration dependence of the fluorescence profiles of 1,8-ANS. Polymer concentrations: 0,  $0.5 \times 10^{-6}$  M, and  $1.0 \times 10^{-6}$  M. [1,8-ANS] =  $1.0 \times 10^{-6}$  M.

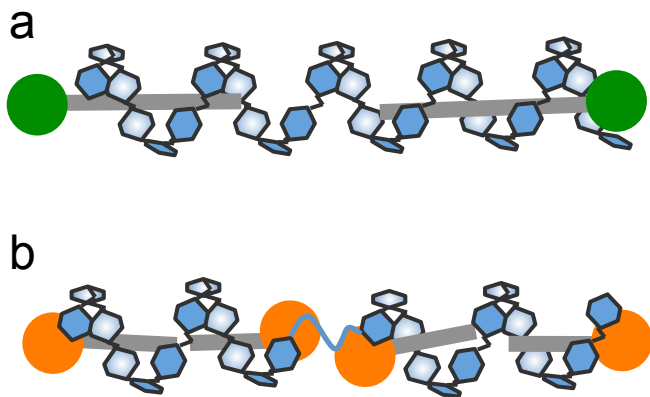


Figure S17 Schematic drawing of the postulated amylose-lipid complexes. (a): the lipids are entrapped in each end of the helical segments of amylose (b): the lipids are entrapped in each end of two amylose helices, which are interconnected by an amorphous amylose linker.

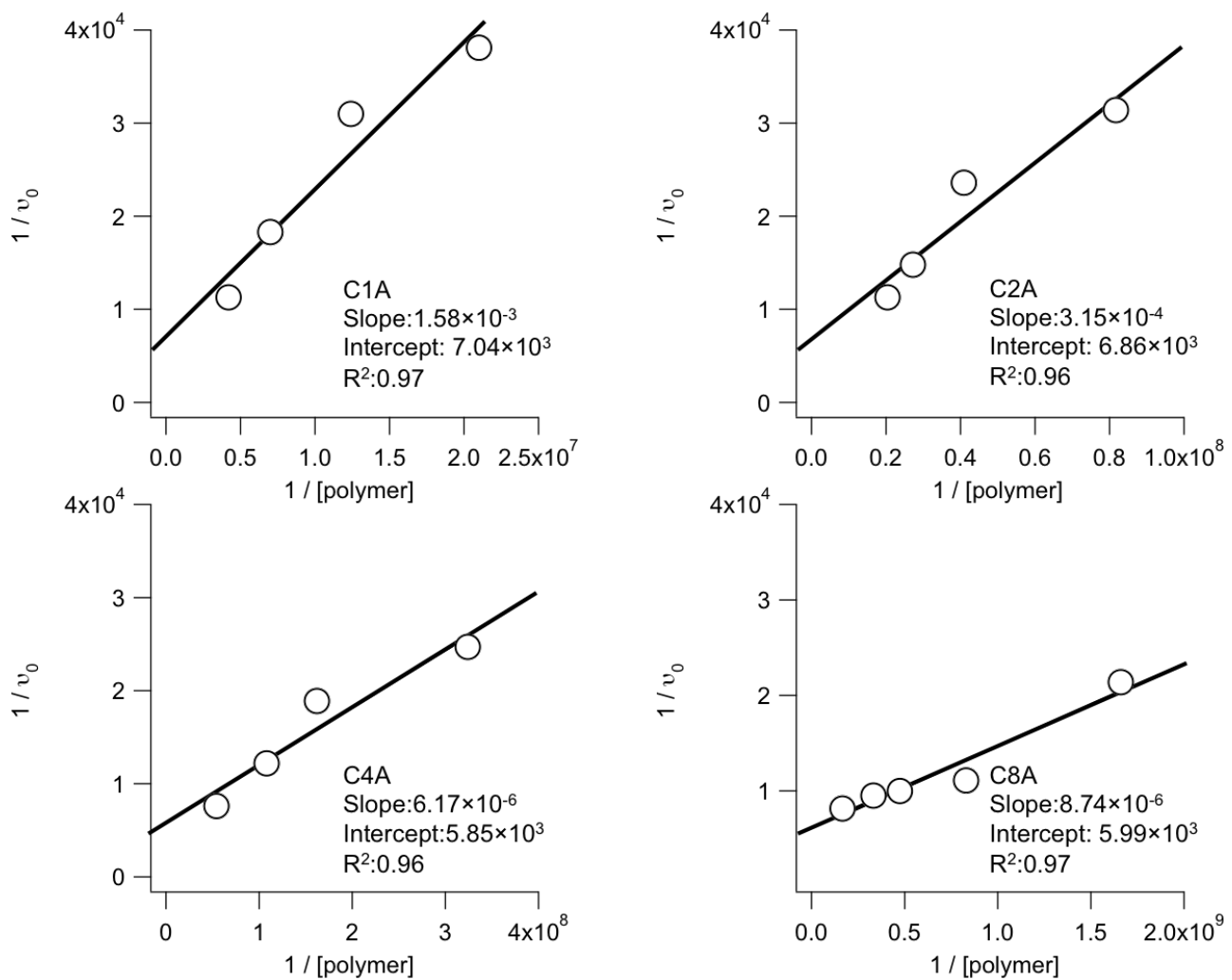


Figure S18 Lineweaver-Burk plots for cationic multi-armed glyco star copolymers.

## Synthesis

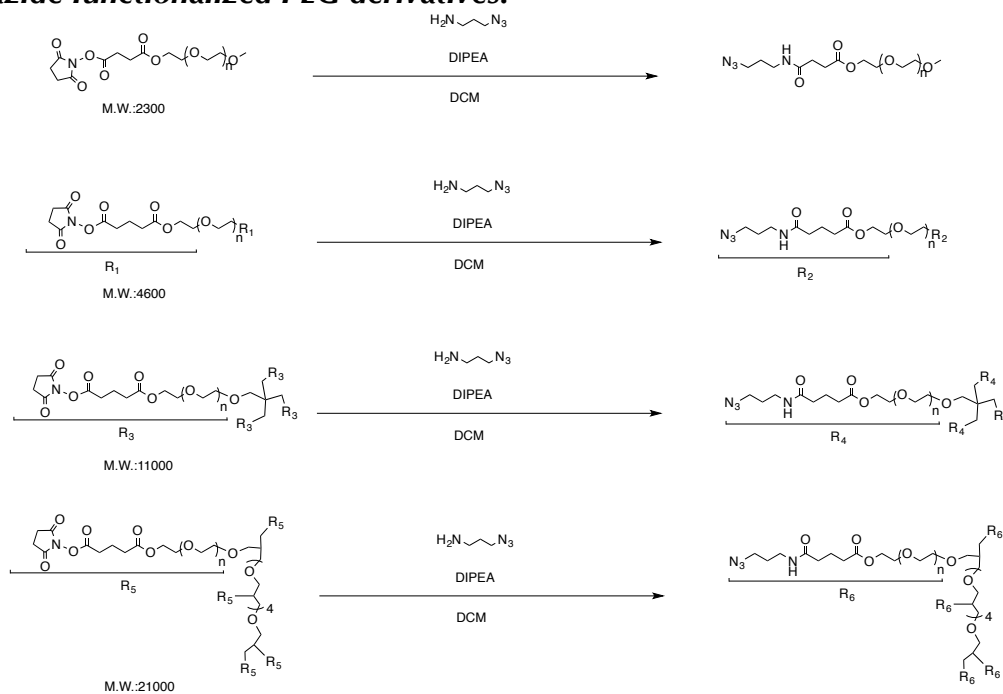
The progress of the reactions was monitored by thin layer chromatography (TLC, Merck254, silica) and the compounds were detected either by exposure to UV or by spraying with a basic solution of potassium permanganate. Flash column chromatography purifications were carried out on silica gel 60 (Kanto Chemical Co. Inc., 40—50  $\mu\text{m}$ ). Nuclear magnetic resonance spectra were run in chloroform-d,  $\text{D}_2\text{O}$  or dimethylsulfoxide-d<sub>6</sub> using Bruker Avance III 400MHz spectrometers to acquire 1H and 13C NMR spectra. Chemical shifts ( $\delta$ ) are expressed in parts per million and are reported relative to trimethylsilane (TMS) or 3-(trimethylsilyl)propionic-2,2,3,3-d<sub>4</sub> acid, sodium salt (TSP) as an internal standard in 1H and 13C NMR spectra, with coupling constants ( $J$ ) expressed in Hertz.

Azide propyl amine<sup>[S5]</sup> and alkyne functionalized maltopentaose<sup>[S6]</sup> was synthesized according to literature procedure.

[S5]: B. Carboni, et al, *J. Org. Chem.* **1993**, 58, 3736-3741.

[S6]: I. Otsuka, et al, *Langmuir* **2009**, 26, 2325-2332.

### Synthesis of azide functionalized PEG derivatives:



Scheme S1 Synthetic Scheme of azide functionalized PEG derivatives

Azide propyl amine (0.11 g, 1.09 mmol) was added portionwise to a solution of mono NHS functionalized PEG (1.00 g, 0.22 mmol, M.W.=2300) and *N,N*-diisopropylethyl amine (0.08 g, 0.65 mmol) in DCM (10 mL) at room temperature. The mixture was stirred for 17 hr at room temperature. The reaction solution was dialyzed against the distilled water in a dialysis membrane (molecular weight cutoff 1000) for 3 days, and lyophilized to yield the solid products.

In a same manner, bis, tetra, and octa azide functionalized multi-armed peg was synthesized from bis NHS PEG(M.W.: 4600), tetra NHS PEG(M.W:11000), and octa NHS PEG(M.W.:21000) respectively.

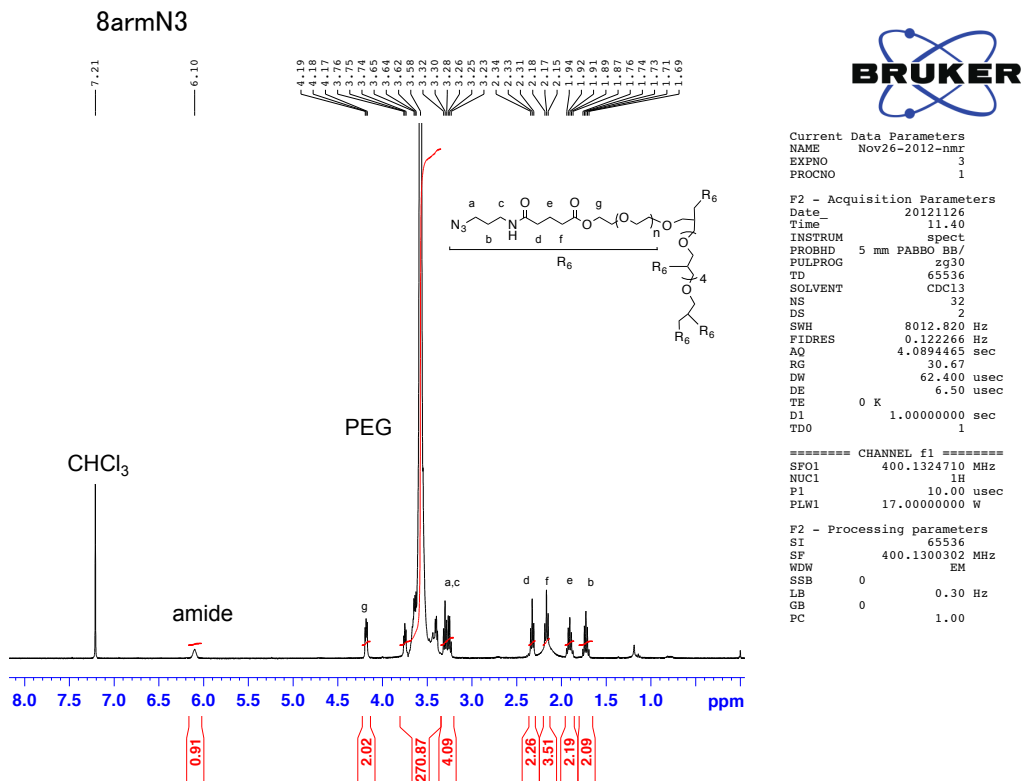


Figure S19 NMR spectra of azide functionalized 8 arm PEG

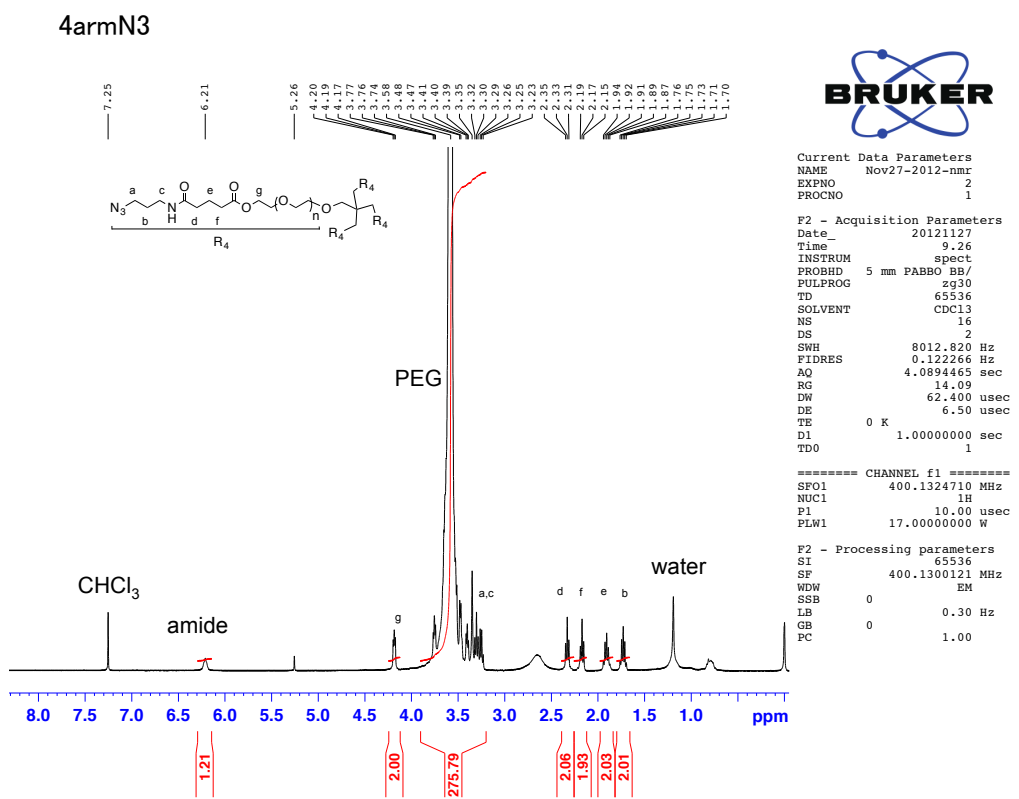


Figure S20 NMR spectra of azide functionalized 4 arm PEG

2armN3

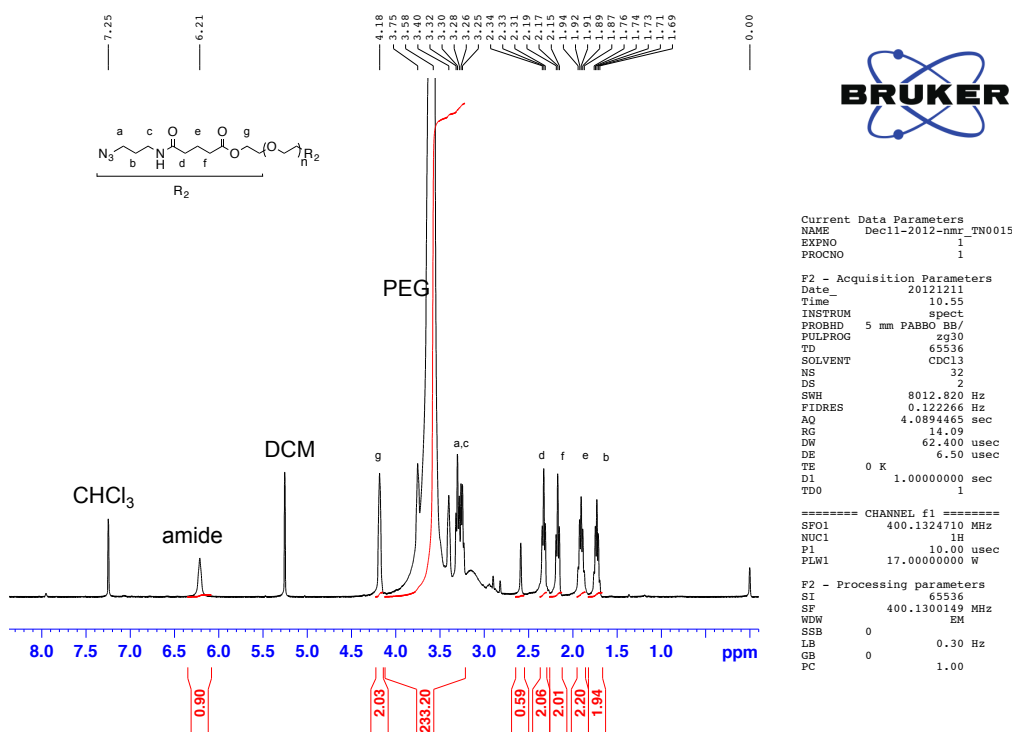


Figure S21 NMR spectra of bis azide functionalized PEG

1armN3

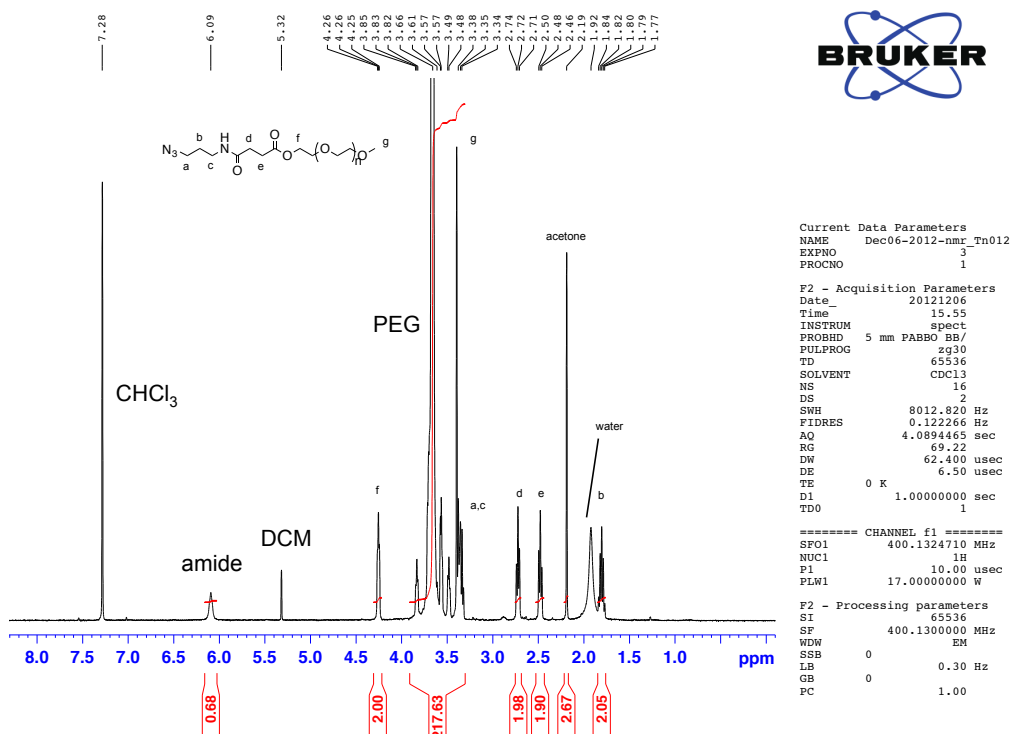
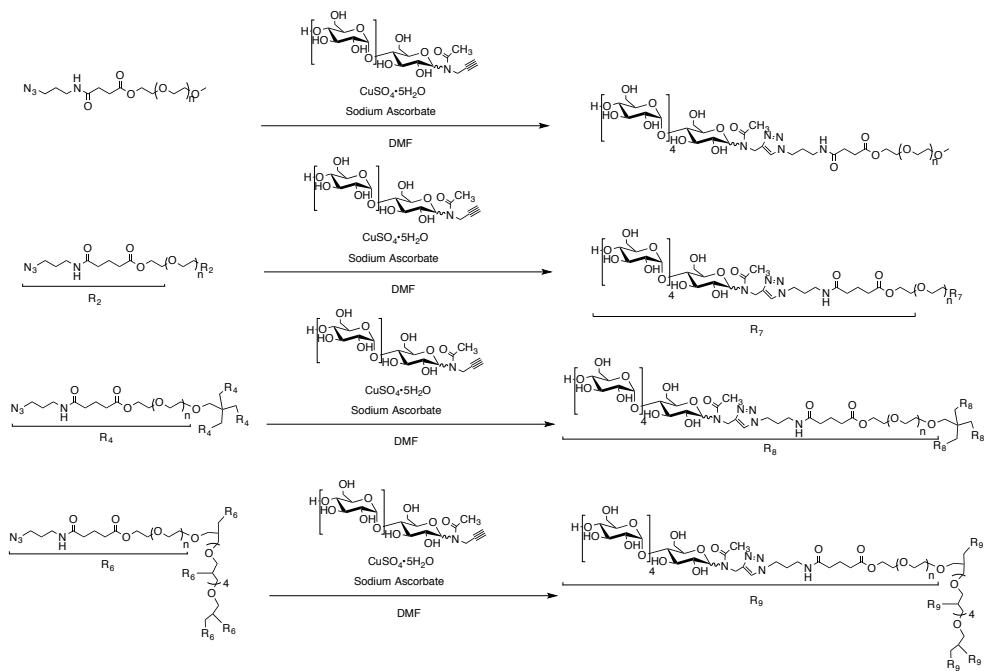


Figure S22 NMR spectra of mono azide functionalized PEG

**Synthesis of Maltopentaose functionalized PEG derivatives:**



Scheme S2 Synthetic Scheme of Maltopentaose Functionalized PEG derivatives

A mixture of mono azido functionalized PEG (0.50 g, 0.11 mmol), copper sulfate pentahydrate (0.006 g, 0.022 mmol), sodium ascorbate (0.009 g, 0.044 mmol) and alkyne functionalized maltopentaose (0.40 g, 0.44 mmol) in dry *N,N*-dimethylformamide (10 mL) were stirred at 40°C for 48 h under an argon. The reaction mixture was cooled to RT. The reaction solution was dialyzed against the distilled water in a dialysis membrane (molecular weight cutoff 1000) for 3 days, and lyophilized to yield the solid products. Bis, tetra, and octa maltopentaose functionalized multi-armed peg was synthesized in a same manner.

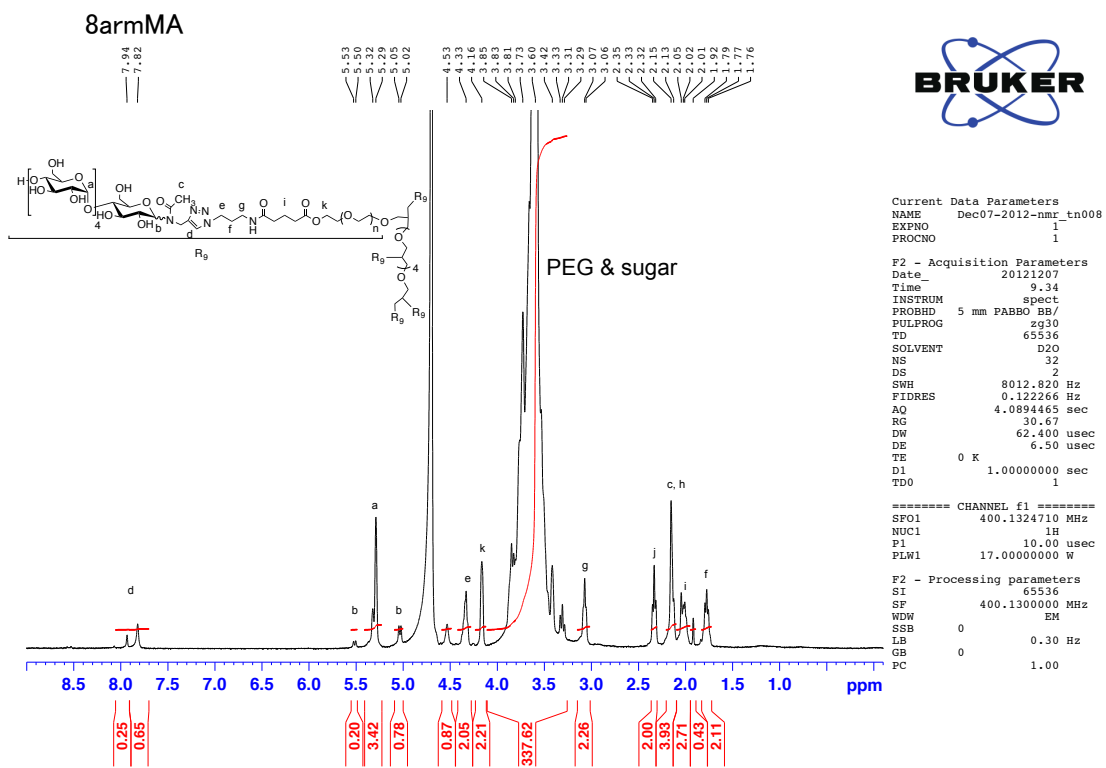


Figure S23 NMR spectra of maltopentaose functionalized 8 arm PEG

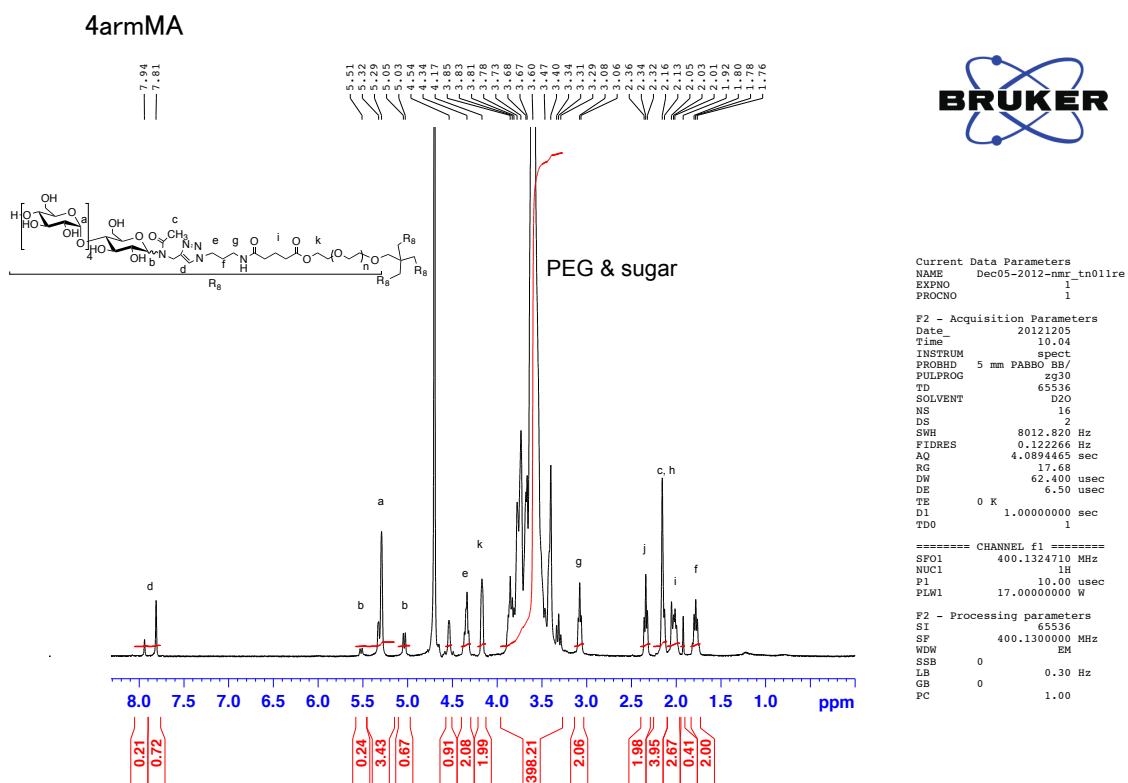


Figure S24 NMR spectra of maltopentaose functionalized 4 arm PEG

### 2armMA

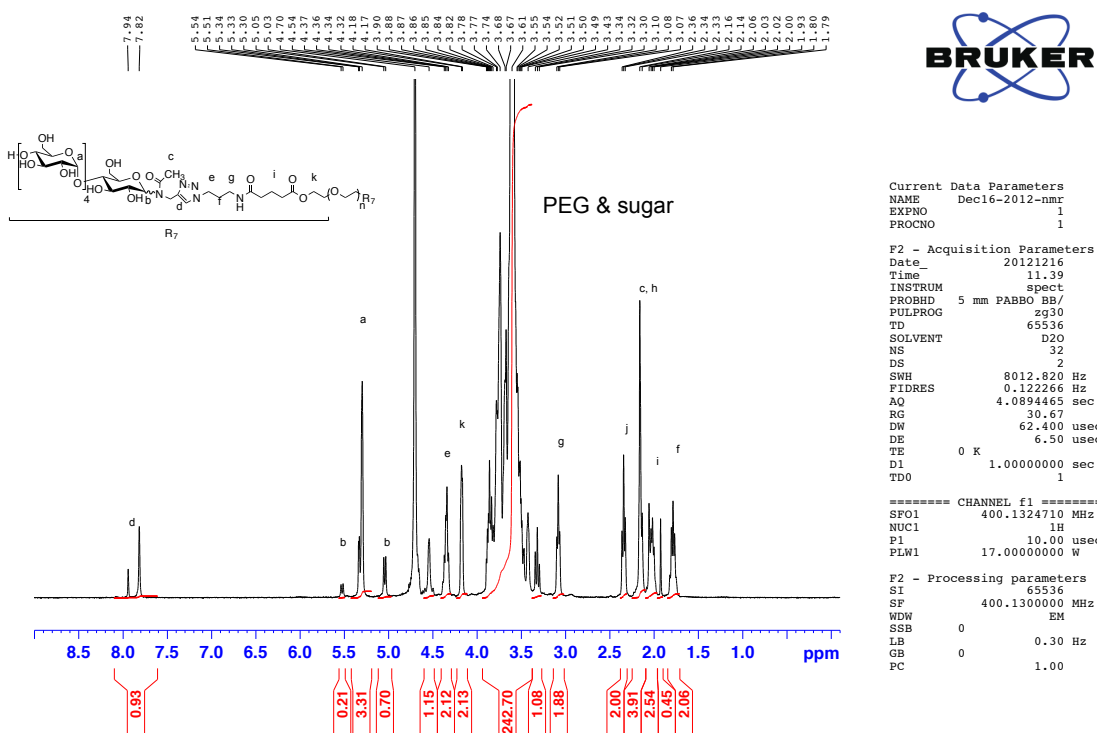


Figure S25 NMR spectra of bis maltopentaose functionalized PEG

### 1armMA

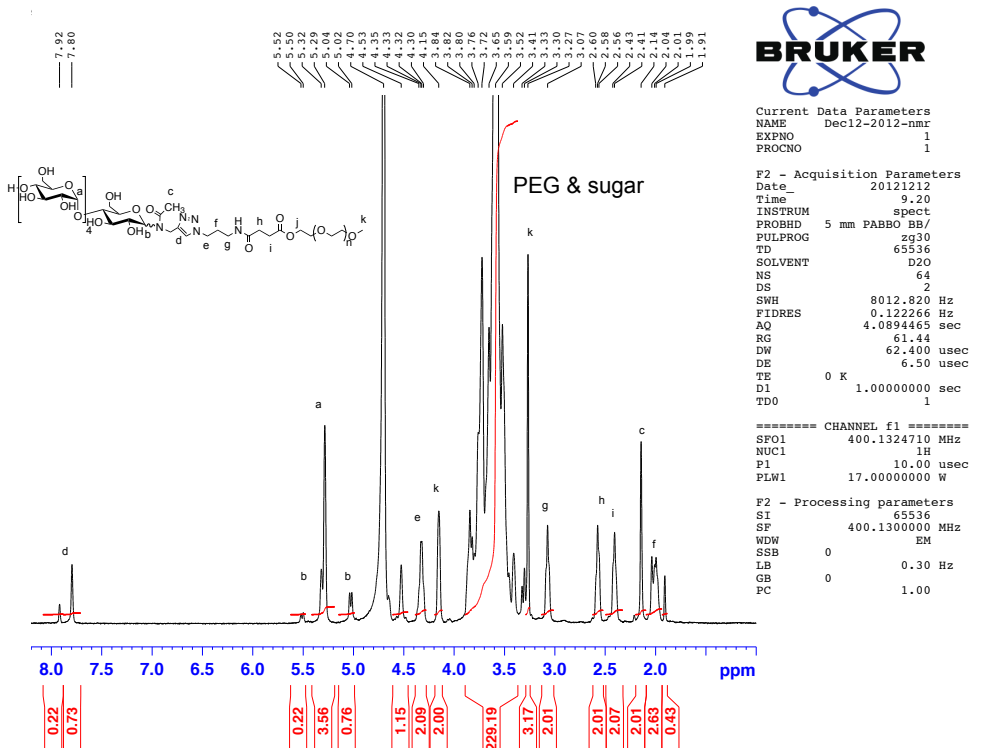
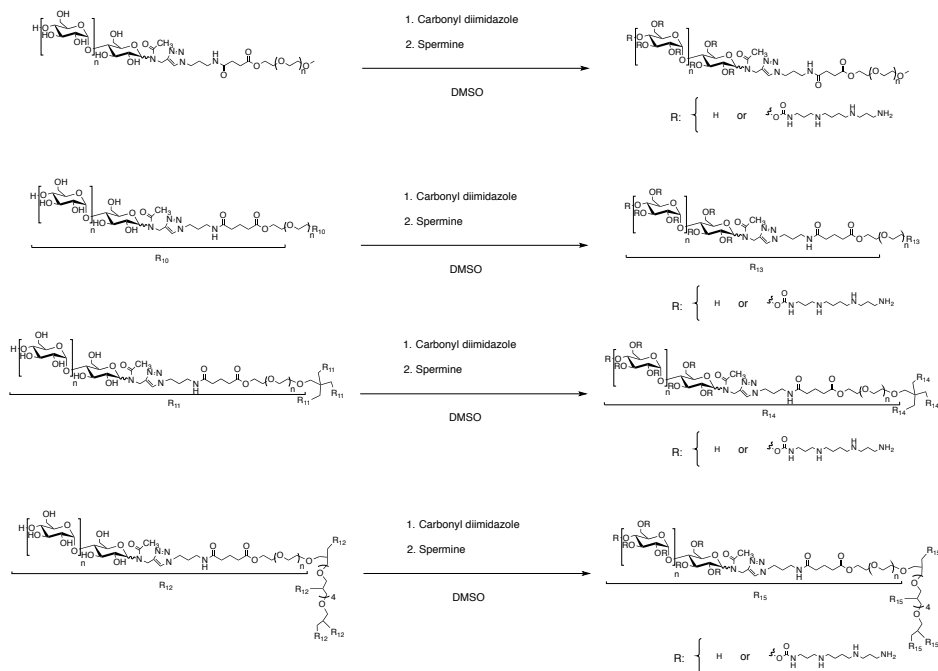


Figure S26 NMR spectra of mono maltopentaose functionalized PEG

### ***Enzymatic polymerization:***

To maltopentaose functionalized PEGs (1 mM), glucose-1-phosphate (100 mM), and adenosine mono phosphate (10 mM) in Bis tris buffer (pH=6.0; 0.1 M), rabbit muscle Phosphorylase b (0.26  $\mu$ M) was added. Then the solution was incubated at 40 °C during the polymerization. The polymerization was monitored by the inorganic phosphate assay. The polymerization was quenched by heating at 100 °C for 5min. The coagulated protein was removed by filtration (0.45 $\mu$ m), and after this, the product was purified by dialysis (MWCO 1000) against distilled water for 3 days. Finally the product was lyophilized.

### Synthesis of spermine functionalized glyco polymers:



Scheme S3 Synthetic scheme of spermine modified multi-armed glyco copolymer and characteristics for multi-armed cationic glyco star copolymers

To a solution of mono arm glyco polymer (0.065 g, 0.31 mmol) in 10 mL of dry DMSO at room temperature under an Ar was added dropwise of carbonyldiimidazole (0.035 g, 0.22 mmol) in DMSO (15mL). The reaction mixture was stirred at room temperature for 5 hour. Spermine (0.44 g, 2.16 mmol) in DMSO (10mL) was added to the reaction mixture, and the mixture was stirred at room temperature for 18 hour. The reaction solution was dialyzed against the distilled water in a dialysis membrane (molecular weight cutoff 1000) for 3 days, and lyophilized to yield the solid products. Other cationic glyco copolymers were synthesized in a same manner.

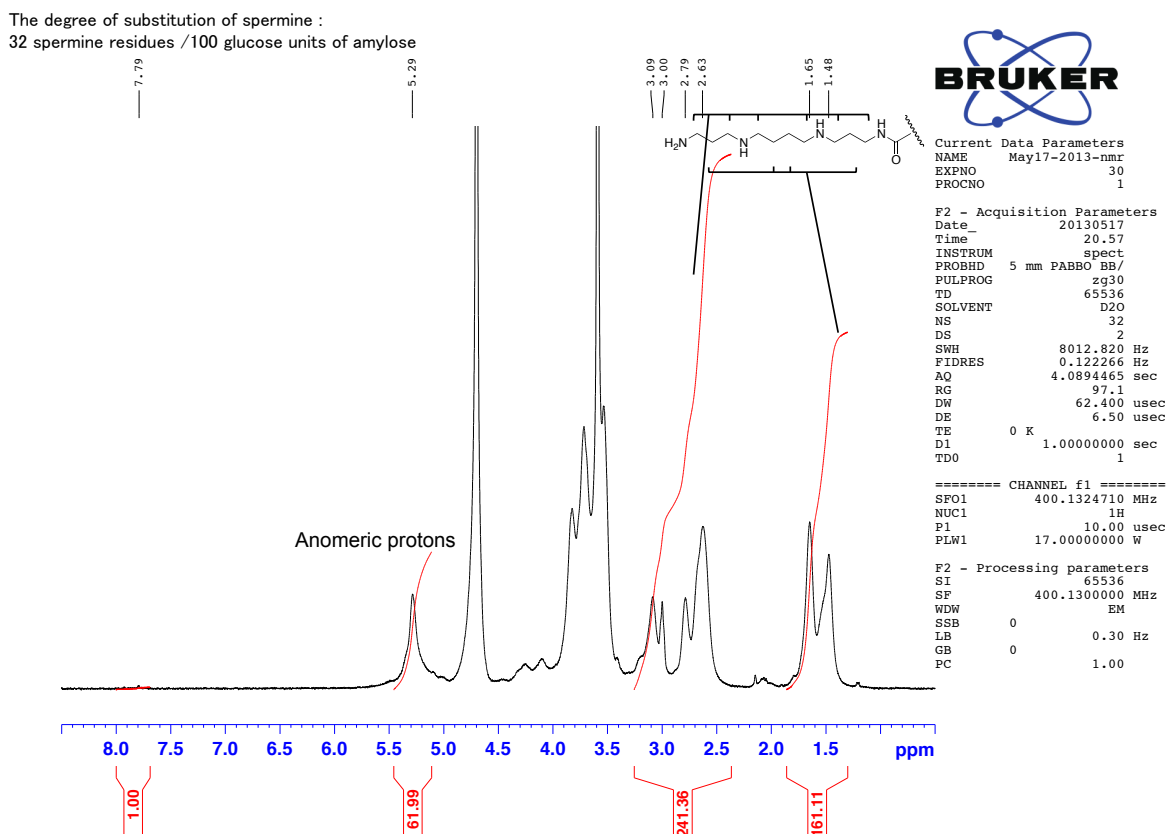


Figure S27 NMR spectra of spermine functionalized 8 arm glyco star copolymer

The degree of substitution of spermine :  
27 spermine residues /100 glucose units of amylose

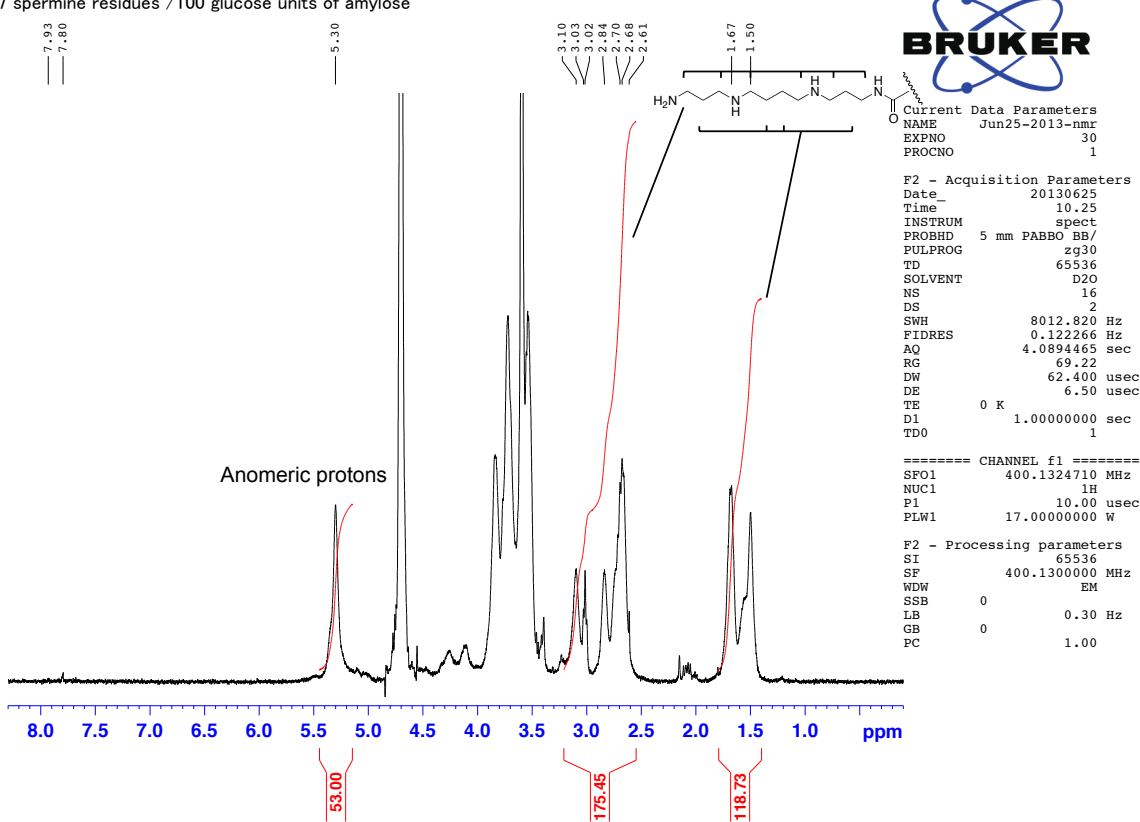


Figure S28 NMR spectra of spermine functionalized 4 arm glyco star copolymer

The degree of substitution of spermine :  
30 spermine residues /100 glucose units of amylose

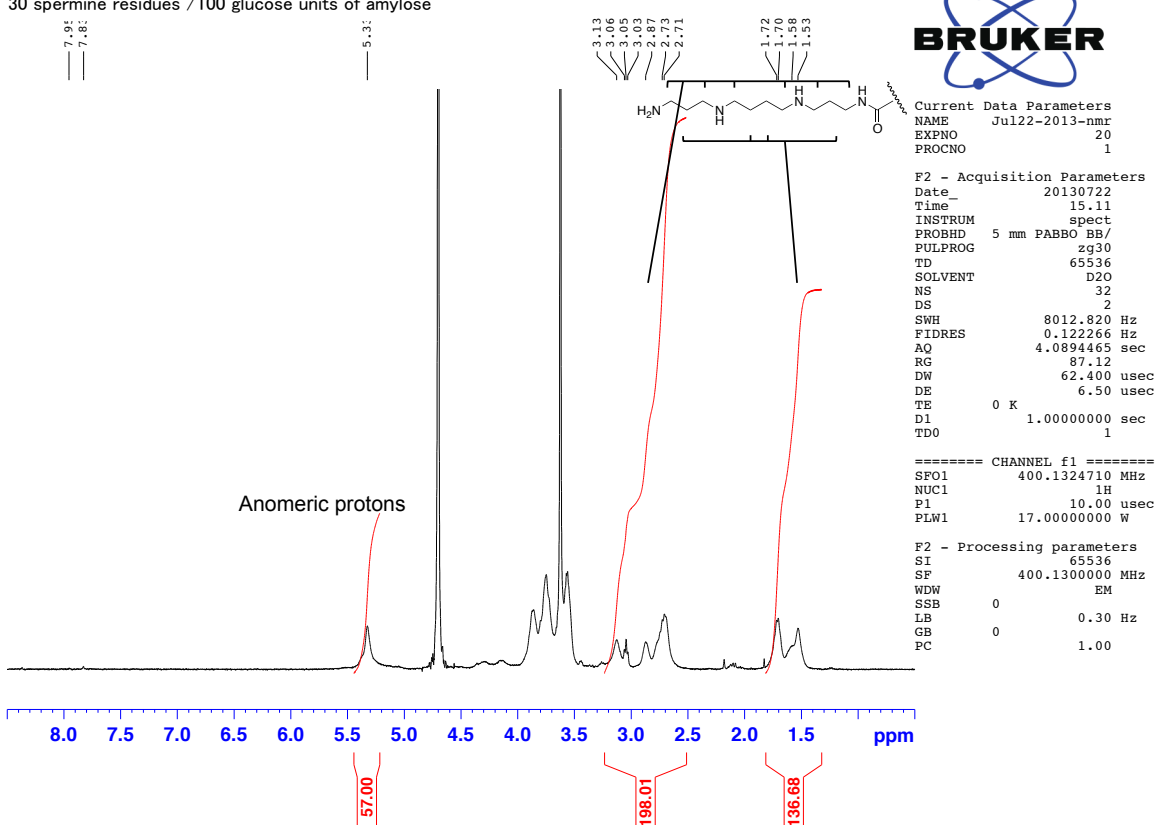


Figure S29 NMR spectra of bis spermine functionalized glyco copolymer

The degree of substitution of spermine :  
31 spermine residues /100 glucose units of amylose

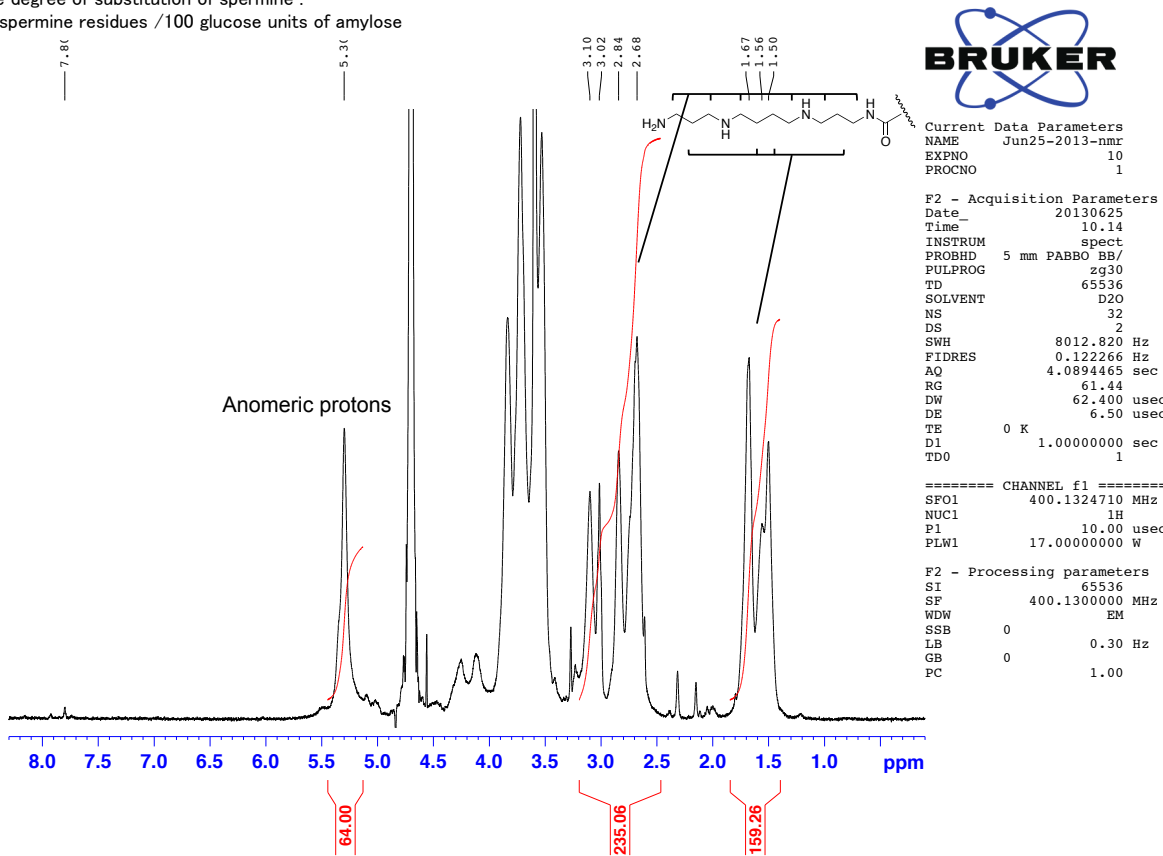
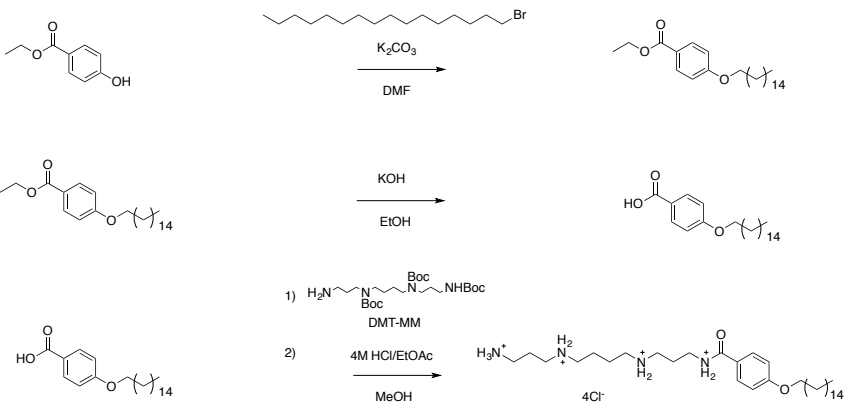


Figure S30 NMR spectra of mono spermine functionalized glyco copolymer

### Synthesis of C16SP:



Scheme S4 Synthetic scheme of C16SP

To a solution of ethyl-4hydroxybenzoate (0.25g, 1.5 mmol) and Potassium carbonate (0.41g, 3.0 mmol in dry DMF (10 mL) was added 1-bromohexadecane (0.55g, 1.8 mmol). The reaction mixture was stirred at 60°C for 6 h under an Ar. The solution was cooled to RT. After removal of solvent under reduced pressure, DCM (30mL) was added. The organic layer was washed with water and brine and then dried over  $MgSO_4$ . The target compound was isolated by column chromatography on silica using DCM : Hexane = 95 : 5 as the eluent to yield 531mg (91 %).

To a suspension of ethyl 4-(hexadecyloxy) benzoate (0.52g, 1.3mmol) in EtOH (50 mL) was added potassium hydroxide (0.67g, 11.9 mmol). The solution was refluxed for 6 h and then cooled to RT. The precipitate was collected by filtration and washed with water to give the desired compound as a white powder (469 mg, 98%).

A solution of 4-(hexadecyloxy) benzoic acid (0.32g, 0.64mmol) in dry THF (3 mL) was added to a solution of tert-butyl (4-((3-aminopropyl) (tert-butoxycarbonyl) amino) butyl)(3-((tert-butoxycarbonyl)amino)propyl carbamate (0.28g, 0.77mmol) and DMT-MM (0.36g, 1.29mmil) in dry THF(15 mL).The reaction solution was stirred at RT for 20h. The solvent was removed under reduced pressure. DCM (20 mL) was added to the residue. The organic layer was washed with water and brine, and dried over  $\text{MgSO}_4$ . Boc protected C16 SP was used without further purification. To a solution of boc protected C16SP in dry DCM (1mL) was added 4M HCl/EtOAc (5mL). The reaction mixture was stirred at RT for 30min. The solvent and volatile compounds were removed under reduced pressure. The residue was washed with DCM to give C16SP (0.30g, 71 % in 2 steps).

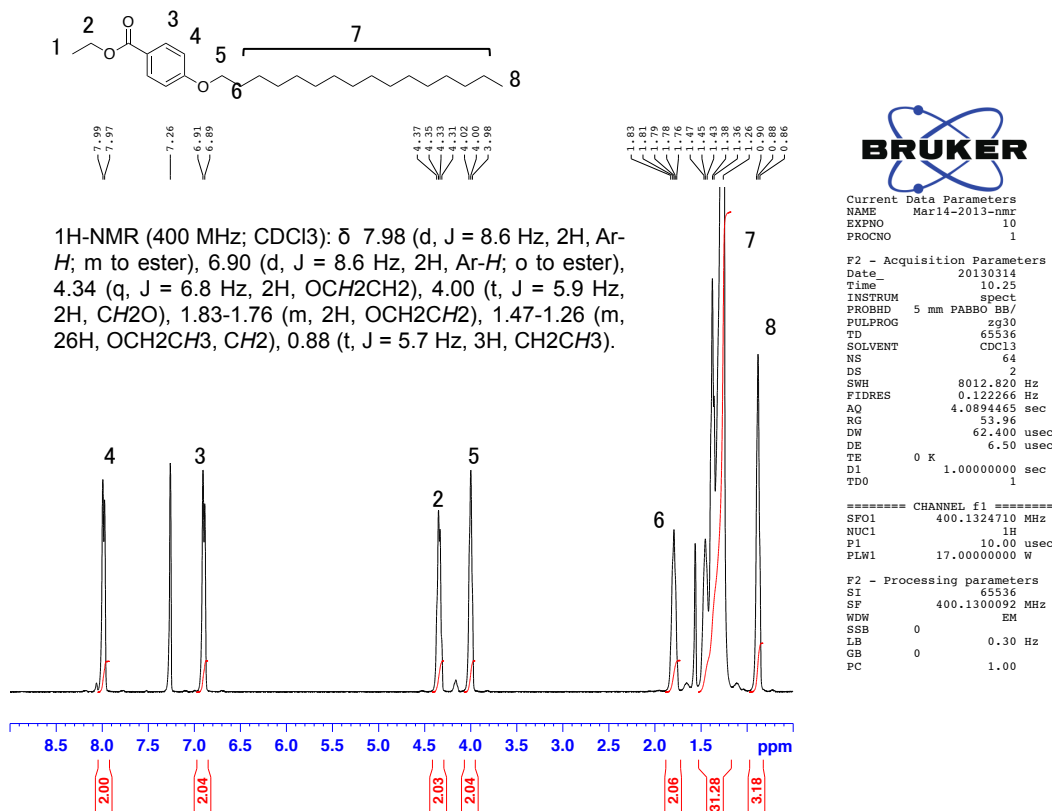


Figure S31 NMR spectra of ethyl 4-(hexadecyloxy)benzoate

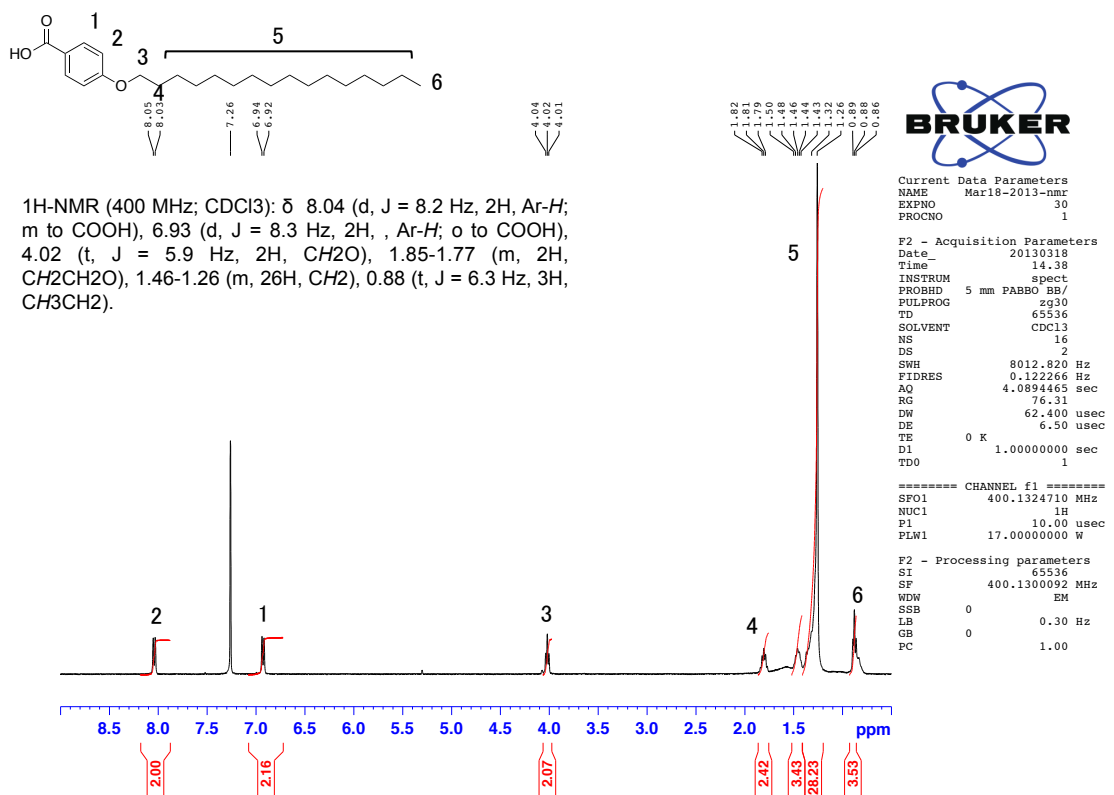


Figure S32 NMR spectra of 4-(hexadecyloxy)benzoic acid

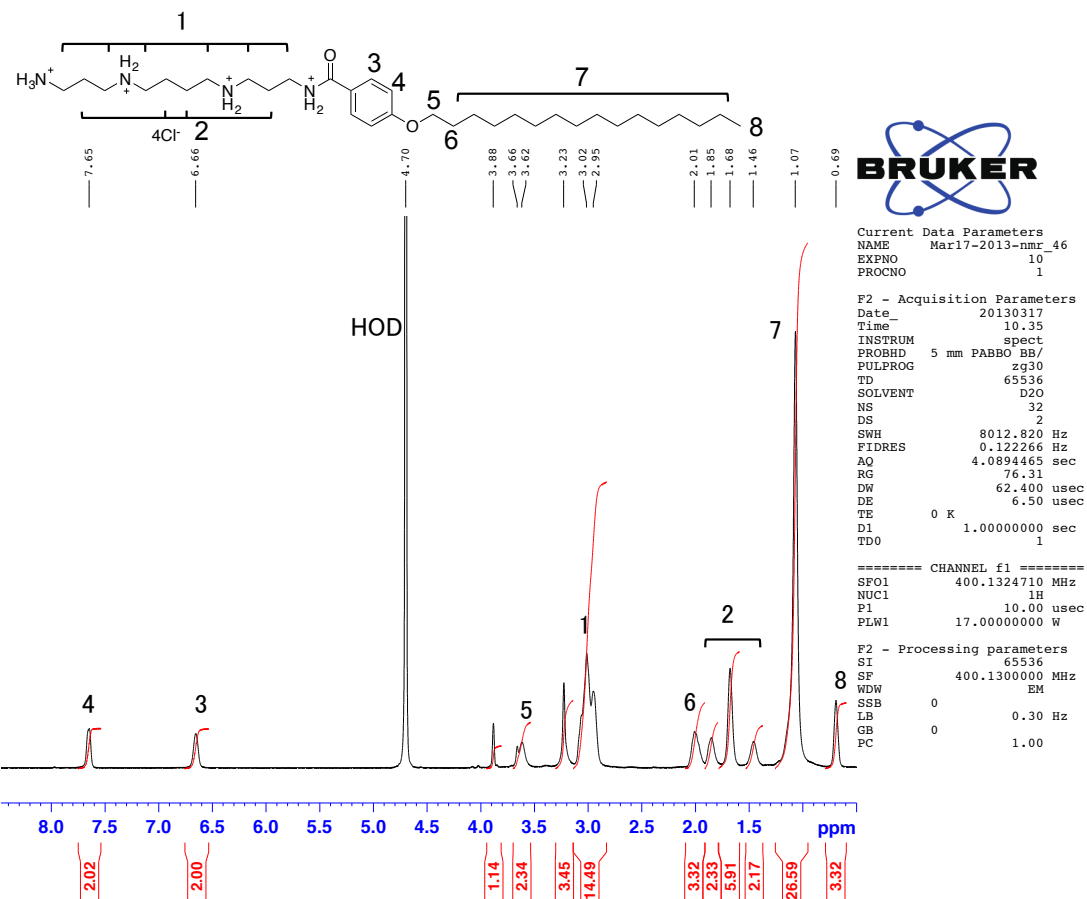


Figure S33 NMR Spectra of C16SP